JOURNAL OF APPLIED PHYSICS

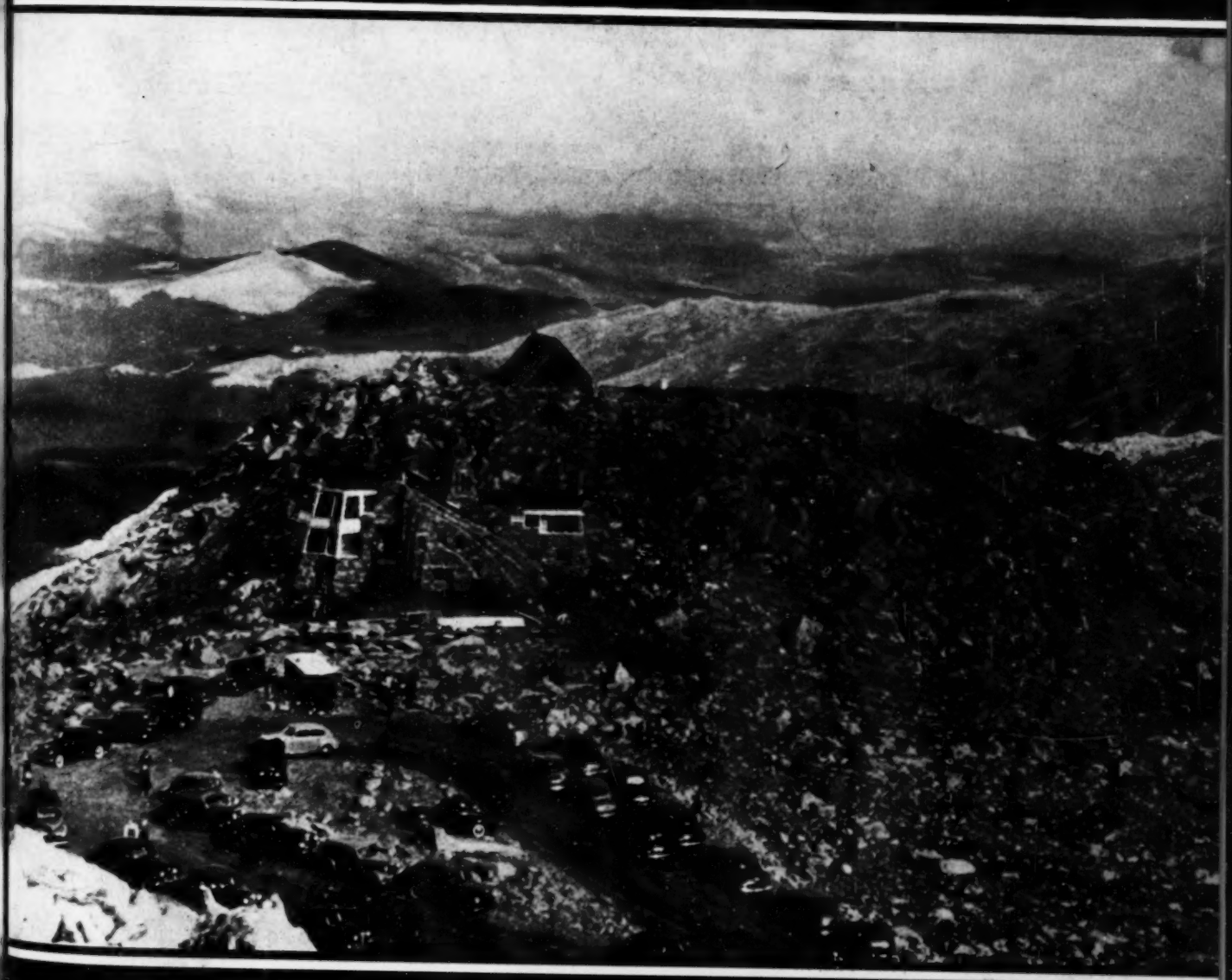

JOURNAL OF APPLIED PHYSICS

Vol. 14, No. 2 FEBRUARY, 1943

In This Issue

Page

Physics in 1942 THOMAS H. OSGOOD 53

Electrostatic Electron Microscopy. II C. H. BACHMAN AND SIMON RAMO 69

Contributed Original Research

Ploughing and Adhesion of Sliding Metals F. P. BOWDEN, A. J. W. MOORE, AND D. TABOR 80

Two-Dimensional Boundary Value Problems in Potential Theory I. S. SOKOLNIKOFF AND R. D. SPECHT 91

Probable X-Ray Mass Absorption Coefficients for Wave-Lengths Shorter Than the *K* Critical Absorption Wave-Length JOHN A. VICTOREEN 95

In Every Issue

New Books 77

Here and There 78

Index to Advertisers xiv

BOARD OF EDITORS

ELMER HUTCHISSON, *Editor*

Associate Editors

FRANCIS BITTER
W. F. BUSSE
S. H. CALDWELL
ROBLEY D. EVANS
SELIG HECHT
W. J. LYONS
MORRIS MUSKAT
THOMAS H. OSGOOD
PAUL E. SABINE
FREDERICK SEITZ
J. R. TOWNSEND
B. E. WARREN
J. B. WHITEHEAD

Publication of the American Institute of Physics

ADMINISTRATIVE STAFF

HENRY A. BARTON, *Director*
MADELINE M. MITCHELL, *Publications Manager*
JOHN T. TATE, *Adviser on Publications*

GOVERNING BOARD

PAUL E. KLOPSTEG, *Chairman*
GEORGE B. PEGRAM, *Secretary*
R. B. DOW
L. A. DUBRIDGE
FLOYD A. FIRESTONE
HARVEY FLETCHER
R. C. GIBBS
K. S. GIBSON
ARTHUR C. HARDY
GEORGE R. HARRISON
HERMANN MARK
A. G. WORTHING
JOHN T. TATE
N. W. TAYLOR
WALLACE WATERFALL

The JOURNAL OF APPLIED PHYSICS, published monthly at Prince and Lemon Sts., Lancaster, Pa., is devoted to physics in its role as the science basic to other natural sciences and to the arts and industries. Previous to 1937 this publication was known as PHYSICS. The JOURNAL OF APPLIED PHYSICS publishes editorials, news of physicists and reviews, as well as technical papers of applied physics.

Manuscripts should be submitted to Elmer Hutchisson, Editor, 172 Fulton Street, Eleventh Floor, New York, New York.

Subscriptions and orders for back numbers should be addressed to Prince and Lemon Streets, Lancaster, Pa. or to the American Institute of Physics, 175 Fifth Avenue, New York, N. Y.

Subscription Price

	U. S. AND CANADA	ELSEWHERE
To members of scientific societies	$5.00	$5.70
To all others	7.00	7.70

Back Number Prices

Complete set: Vol. 1, July, 1931–Vol. 13, 1942–**$80.50**
Yearly back number rate: **$7.70**
Single copies: **$0.70** each.

Changes of address and proofs should be addressed to the Publications Manager.

Advertising rates supplied on request. Orders, advertising copy and cuts should be sent to the American Institute of Physics.

Entered as second class matter January 22, 1937, at the Post Office at Lancaster, Pennsylvania, under the Act of March 3, 1879. Accepted for mailing at the special rate of postage provided for in the Act of February 28, 1925, authorized May 2, 1932.

Copyright 1943, by the American Institute of Physics.

Journal
of
Applied Physics

Volume 14, Number 2 February, 1943

Physics in 1942

BY THOMAS H. OSGOOD

Michigan State College, East Lansing, Michigan

I. CRYSTALS AND PHOTONS

NEARLY twenty years ago, alpha-particles from natural radioactive sources and protons resulting from the disintegration of light elements were counted by scintillations, luminescent points of light which are visible under a microscope when such particles impinge on a screen of zinc sulfide. As gracious expressions of professional courtesy, workers in the field of radioactivity would sometimes exchange specimens of the zinc sulfide which they used in their experiments. In 1924, the late Lord Rutherford received such a gift from a friend in Germany. Upon examining the powder, he found it too coarse for his liking, and therefore directed his laboratory assistant, Crowe, to grind it to a finer size in a mortar before sprinkling it on the castor-oil smeared glass plate which served as a screen. When this was done, it was a source of keen disappointment to Rutherford and all who participated in his experiments to find that the new screen was quite unsatisfactory, in as much as only a small fraction of the incident alpha-particles and protons produced observable scintillations. After some correspondence, a new sample of zinc sulfide was received from the same source, with a suggestion that the material be used in its coarser form. This time it proved to be thoroughly satisfactory; but there remained the unanswered question, why did the grinding destroy the luminescent properties of the crystals?

In the intervening years, experimental and theoretical work on photo-conductivity and related topics have added enormously to our understanding of the behavior of atoms, ions and electrons in crystals, and make it possible to give a fairly satisfactory answer to the question now. Complete summaries of recent work, and of the present knowledge of solids, are available in two books by Mott and Gurney[1] and by Seitz,[2] as well as in a series of papers by many authors, stemming from the early work of Pohl.

A qualitative answer to the twenty-year-old question will give at least an inkling of the concepts which enter into one aspect of the modern theory of solids, though it can give little idea of the scope of the theory as a whole. First it is necessary to mention that studies of the photo-conductivity of crystals have led to a clear understanding of the relations between crystals and photons, and have provided a good explanation of the coloration and darkening of crystals under the influence of light—matters which are of extraordinary importance in the theory of the photographic process. One of the most significant observations is that crystals of

the alkali halides, for example, when heated in an atmosphere of their proper alkali vapor, can absorb an excess of these alkali atoms, even in chemically distinguishable amounts. The absorption is not a surface effect, so there must be within the crystals some sorts of vacancies, known as trapping centers where these excess atoms can reside.

Now all specimens of zinc sulfide are not fluorescent, nor is all zinc sulfide photo-conducting. To prepare the fluorescent variety, the ordinary sulphide is heated alone, or with a small amount of another heavy sulfide, such as copper, manganese, or silver. This treatment not only renders the crystals fluorescent, but at the same time causes them to become photo-conducting. It appears, then, that there is a close connection between the two effects. As the heat treatment proceeds, the zinc sulfide decomposes slightly, and a preferential evaporation of sulphur atoms takes place from the surface. An abnormally large number of zinc atoms is thus left behind in the solid, and metallic atoms of the accompanying heavy sulfides may also infiltrate to the crystal. These excess foreign or zinc atoms diffuse throughout the crystal, perhaps as positive ions, but more likely as neutral atoms. If some are in the form of ions, there must be a corresponding number of free electrons wandering, or trapped, in the lattice, for the crystal is electrically neutral. Be that as it may, the luminescence of the crystal under the influence of ultraviolet light or of flying particles is definitely conditioned by the presence of these excess zinc atoms or ions, which may be raised by a local stimulus to excited levels. During the return to their normal levels, the light which constitutes fluorescence or a scintillation is emitted.

However, the internal economy of such a luminescent crystal is sensitive to external disturbances. Even the mechanical forces involved in crushing the crystals in a mortar, or the heating which may be a secondary effect accompanying rupture, may be enough to cause the excess zinc atoms or ions in the finely powdered crystal to form small aggregates of zinc metal, which will be definitely anchored at one spot in the crystal. Indeed, the process is probably closely akin to that whereby a photographic film, upon exposure to light, or upon being pinched, undergoes local electrolysis, forming free bromine and numerous tiny bunches of free silver atoms which are the black grains in the developed emulsion. Once this has happened in zinc sulfide, the excess solitary metallic atoms are no more, and scintillations will be produced but rarely by impinging alpha-particles or protons.

II. THERMAL DIFFUSION

Different kinds of molecules can usually be separated from a mixture by combinations of physical and chemical means. With the discovery of isotopes, and with the recognition of their importance in the study of artificial radioactivity, the need has grown more urgent for a method of separation involving physical means alone. While the problem has become more pressing, it has also become more difficult, because the only differences between isotopes are differences of mass amounting usually to not more than a few percent. Maxwell's demon could do the trick, but something much more practical is required. A mass spectrograph can also achieve a complete separation, but with a yield only about one-ten-millionth of what is desired.

Several new methods have been tried in the last twenty years, many achieving partial success.[3] Perhaps the most promising at the moment is that involving thermal diffusion. This is not the same effect as the ordinary diffusion process which is described in elementary accounts of the kinetic theory of gases, and which occurs and is manifest in a gas mixture maintained at a uniform temperature. By virtue of the process of ordinary diffusion a local concentration of a foreign gas, introduced artificially into a gas-filled chamber, will distribute itself uniformly within the limits of statistical error throughout the whole volume, merely because all the molecules are moving. On the other hand, thermal diffusion shows itself in a mixture of different kinds of particles which is kept at a non-uniform temperature. For the sake of simplicity, let the gas mixture under consideration be confined between two vertical parallel walls H and C, a short distance apart. Let H be heated and C cooled. Then thermal diffusion creates a concentration gradient perpendicular to H and C, the lighter

particles being the more numerous near the wall H. Strong convection currents then come into play, carrying the abnormal concentration of light particles upward and the abnormal concentration of heavy particles downward. Thus, after a time, the upper part of the enclosure will be over-populated with lighter particles, the lower part with heavier particles, whence these "fractions" can be drawn off by appropriate means.

Unfortunately, this argument amounts to nothing more than a statement of the facts of the case; as an explanation it appears to be entirely illusory, for nearly all writers on the subject are emphatic in their statements that an explanation of the phenomenon cannot yet be expressed in simple terms. In estimating the success with which the separation of a binary mixture of molecules of dissimilar masses may be carried out it is customary to calculate[4] the value of a thermal diffusion factor α, which connects the coefficient of ordinary diffusion with the coefficient of thermal diffusion and with the concentrations of the two types of particles whose separation is desired. The expression for α in terms of the fundamental characteristics of the mixture involves, in addition to the masses of the constituents, a function which depends on the law of force which is assumed to be operative between the particles. If a spherically symmetrical power law of repulsion is considered, such that the force between a pair of particles is inversely proportional to the nth power of their distance apart, then α is found to contain a factor $(n-5)$. Hence it follows that for $n=5$, that is, for what are known as Maxwellian particles, the thermal diffusion factor α is equal to zero. Therefore, for such particles, no separation by thermal diffusion is possible. It also follows that the concentration gradient between the walls H and C mentioned above may be reversed in direction, depending on whether n is greater than 5 or less than 5. The simplest available derivation of the general shape of the function representing the diffusion factor is to be found in a note by Frankel,[5] who employs dimensional analysis for the purpose. The factor has also been interpreted in a somewhat different fashion by Grew,[6] whose experiments show the reversal of sign in the separation of mixtures of varying proportions of ammonia and neon.

It is, of course, certain that the forces between molecules are not in general spherically symmetrical nor describable by an inverse power law. Nevertheless, the closeness with which such a law approaches the truth may be gauged by the accuracy with which it can be used to predict a thermal diffusion factor which can be compared with an experimental value. In the case of neon, whose force field should, by any elementary argument, be spherically symmetrical, the agreement between theory and experiment is only moderately satisfactory. In the case of methane, whose force field is known not to possess the required symmetry, the agreement is poor. A further difficulty arises because the simple assumption of a spherically symmetrical field of force leads to a value of α which is independent of temperature. Experimental results show that this is not even approximately true.

In spite of the many defects of the theory, the process of thermal diffusion is in practice an effective separator of isotopes. Clusius and Dickel, whose work is mainly responsible for the renewed attention which is now being paid to this subject, used a multiple-tube unit with an effective length of 36 meters, and obtained from ordinary hydrogen chloride light and heavy samples of chlorine which were about 99.5 percent pure. Since the method is applicable also to liquids, it will no doubt be used by those who seek to develop practical sources of atomic energy in an effort to separate the priceless 235 isotope from ordinary uranium.

III. THE NUCLEUS

The exploration of the atomic nucleus is not exploration in the true sense of the word. No one can look into a nucleus to see what is there. Rather, the problem is one of deriving a plausible, but in the first place tentative, structure, and then seeing how it withstands various tests that can be applied to it. The process might be likened, indeed, to the task of a geographer of the middle ages who attempted to describe a foreign country, its people, and its physical features, solely on the basis of what goods were carried to it and from it in ships.

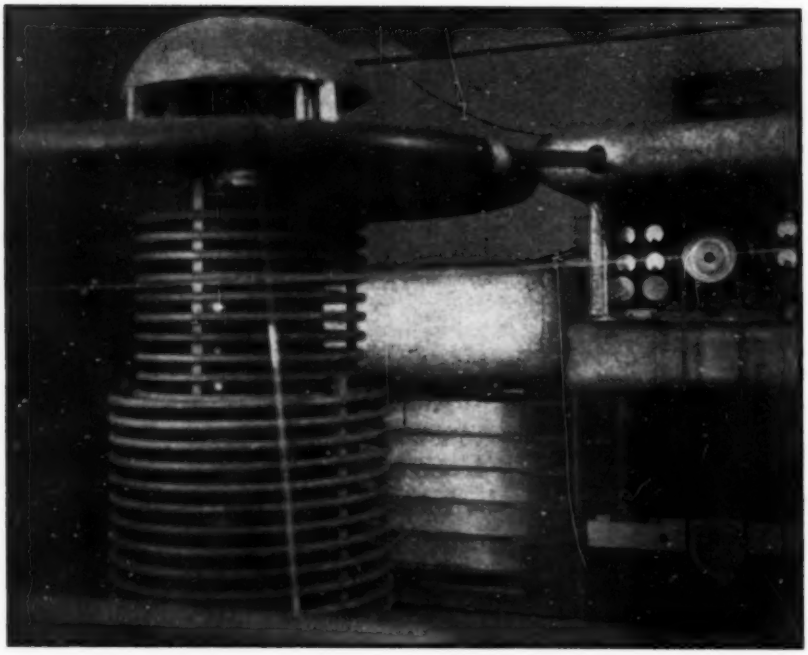

FIG. 1. The vertical accelerating tube, guarded by external metal rings, of the voltage quadrupling outfit used by Ragan, Kanne, and Taschek at the University of Wisconsin. In the background is a bank of condensers and the power supply unit for the arc. (Courtesy of R. F. Taschek.)

There are two parts in the problem of nuclear structure: First, what is a nucleus composed of; second, how is it held together? The answer to the first question is now fairly definite, but the second requires much more research. The forces which are familiar in the laboratory, and upon which the operation of most laboratory instruments depends, forces like those described by Coulomb's law, are still in control when atomic distances of the order of 10^{-8} or 10^{-9} cm are involved. But at distances only one-ten thousandth as great it is not surprising that new types of forces appear. These new forces are what hold the components of the nucleus together. They come into play only when the components approach very close to one another. In technical language, we are interested in the proton-proton and proton-neutron interaction. The most obvious way of finding out about such interactions is to let protons be scattered by other protons or neutrons by protons and so on. By varying the speed of the incident particles the closeness of approach can be varied, and the short-range forces can be found as functions of the distance of separation. The investigation of the scattering of protons by protons has been going on for several years, but only in a few places because of the complexity of the apparatus required to provide the necessary stream of fast-moving particles. The general nature of the proton-proton forces is known up to incident proton energies of about 2 Mev. A great deal of a more detailed nature remains to be discovered. Experiments of half a dozen years ago showed that the scattering of protons by hydrogen, that is by other protons, was far from what could be expected from a simple Coulomb law of force. The scattering was such as might occur if the repulsive Colomb force, operative at comparatively large distances, changed rather suddenly into a strong attractive force, when the distance between the particles was of the order of 10^{-13} cm. Now there must be some critical distance (for some particular velocity of the incident protons) at which these two types of force compete, as it were, for control of the scattering process. Should an incident particle pass just outside this critical distance, it will be scattered normally by the Coulomb field; but should it pass just inside, it will be whipped around the target nucleus and will suffer a deflection which differs considerably from that which occurred in the former case. There will therefore be a scarcity of scattered particles at some definite angle with respect to the incident beam, for some particular energy of incidence, which must, however, be

large enough to bring true nuclear forces into play. This minimum in the scattering curve has been shown to lie at 45° for 400-kev protons, but until Ragan, Kanne, and Taschek[7] studied the region in detail the available information was only approximate.

The space-variation of the short-range nuclear forces of which we have spoken cannot, it is found, be described by a simple power law such as r^{-n}. The variation may not even be continuous. Probably the most successful and compact way of representing these forces is to specify what kind of a potential well they are equivalent to. For example, Breit[8] and his co-workers in 1939 published an analysis of proton scattering up to that date, and concluded that the results could be represented over a range of 2 Mev by supposing that each proton behaved as a square "potential well" superposed upon an existing Coulomb field. Unfortunately, the relevant data were not able to give an unambiguous estimate of the shape of the well; a considerable latitude had to be permitted. Now the new observations of Ragan, Kanne, and Taschek remove the ambiguity. With a high voltage generator at the University of Wisconsin they studied the scattering of protons by hydrogen in the region 200 to 300 kev. A view of the accelerating tube of this outfit, which has already been described in the literature, is shown in Fig. 1, and the pumping and detecting systems, situated a short distance below the accelerating tube, are seen in Fig. 2.

The reasons for choosing this range of energy for particular study are as follows. On either side of the minimum referred to above, that is, about 300 kev, or about 500 kev, the scattering is particularly sensitive to the shape of the potential well which is chosen to represent the proton. Hence, an accurate determination of the amount of scattering in one or both of these neighborhoods will give information from which a correct choice can be made of the well parameters. At the time of their theoretical work, Breit, Thaxton, and Eisenbud could not decide whether a well of width $2e^2/mc^2$ and 10.5 Mev deep, or a well three-quarters as wide and nearly twice as deep represented the results the better. Both gave the same scattering at voltages around 2 Mev, and the scattering at lower voltages was not known precisely enough to make a distinction between the two well-forms possible. The new work from the University of Wisconsin, even though difficult to perform with the necessary accuracy because of the low penetrating and ionizing power of the low-energy protons, decides conclusively in favor of the potential well 10.5 Mev deep and $2e^2/mc^2$ across. This is, however, not the only type of potential well which can be made to fit the observed data. Others have been

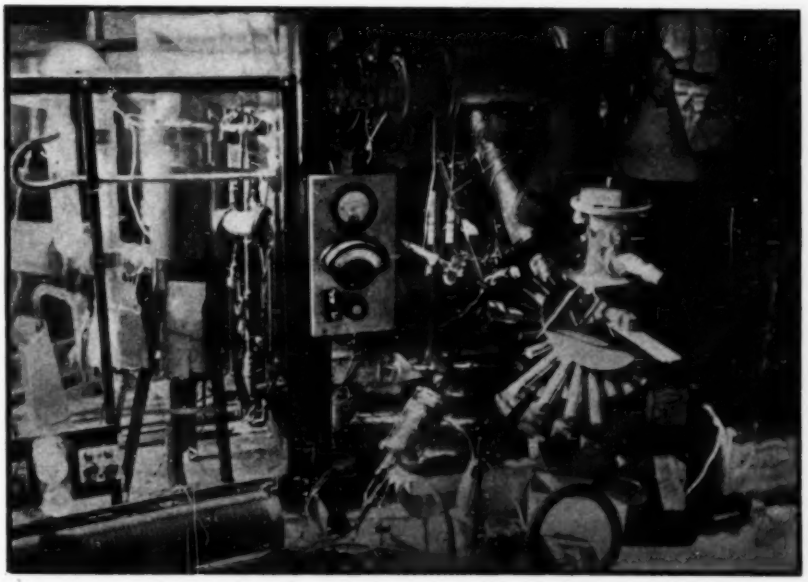

FIG. 2. The spider-like unit on the right is one of the scattering chambers used by Ragan, Kanne, and Taschek. By changing the detector from one arm to another, protons can be observed scattered at various angles from the primary beam, which comes down the large inclined tube behind the chamber. Part of the pumping system is seen at the left. (Courtesy of R. F. Taschek.)

tried, with moderate success. But the problem does not end here. With a knowledge of proton-neutron interaction as well, binding energies, and then masses can be calculated for such particles as He^3 and He^4. If the assumed potential well for the proton leads to the wrong result for these masses, then the constants describing the potential well must be further modified, or a new shape must be tried. The first attempts are naturally made with the simplest forms of well which offer some prospect of success.

The interaction between pairs of elementary particles, such as proton-proton or proton-neutron, are known to be of very nearly the same magnitude. Nevertheless, the theoretical bases on which the detailed calculations of nuclear structure rest amount to little more than a series of assumptions, in need of being tested. If an experimental result is in agreement with any one set of assumptions, the validity of the others may be ruled out, but this agreement, in itself, does not imply the absolute correctness of the hypotheses with which the agreement is found. Experimental work thus proceeds asymptotically, as it were, towards a complete understanding of these short-range nuclear forces. The time is not ripe for a critical experiment which can solve the problem completely, but during the last year several contributions have been made towards the solution of certain aspects of the problem. For example, Carroll[9] has studied the interaction of slow neutrons with protons, using as target material the hydrogen nuclei in a series of hydrocarbons. This has a bearing on the prediction made by Fermi that the cross section under such conditions is influenced by molecular binding. As typical results, Carroll found the cross section of the proton to slow neutrons to be 32×10^{-24} cm^2 for hydrogen gas, and 49×10^{-24} cm^2 for gaseous butane, thus showing that the effective target area per proton increases with increasing complexity of the bombarded molecule. In a paper published a few months ago, Tatel[10] reported an investigation of the protons scattered by high energy neutrons. For experimental convenience, of course, the neutrons were flung at the more or less stationary protons, some of which recoiled under the influence of close collisions, and were detected in ionization chambers. He found that the scattering, referred to the center of gravity of the system of particles, was isotropic, within the ten percent accuracy of his experiments. Such a result is interesting because of its relation to the earlier theoretical work of Rarita and Schwinger.[11] These two authors worked out the consequences to be expected in proton-neutron scattering on the basis of three different assumptions. One of these assumptions, which predicted asymmetrical scattering, now appears to be ruled out.

When theory and experiment concern themselves with scattering by very complicated nuclei, a much more general point of view has to be taken. No longer can the details of the process be considered separately; a statistical or thermodynamic treatment is required, in which the heavy scattering nucleus is considered to possess some of the attributes of a drop of liquid. Such a nuclear model has already had some success in the interpretation of the results of nuclear fission. When it is applied to the scattering of neutrons by lead, an energy spectrum of the inelastically scattered neutrons can be predicted. Several years ago, Weisskopf predicted that fast neutrons, all of one velocity, incident upon a heavy element would be scattered inelastically in such a way that the neutrons, after scattering, should show a Maxwellian distribution of velocities. This point has been tested by Dunlap and Little[12] using neutrons from the D−D reaction with an energy about 2.5 Mev. The distribution of scattered neutrons turns out not to be Maxwellian, but to have a much greater proportion of high energy particles than a classical distribution would have. The reason for expecting a Maxwellian distribution is that the moving neutron is presumed to be captured temporarily by the scattering nucleus, then ejected like a molecule evaporating from a warm drop of liquid. It seems more likely now that the re-emission of a neutron takes place, or may take place, before "thermal" equilibrium has been attained in the nucleus, and that the scattered neutron emerges from the temporary nucleus at some point where a fortuitous concentration of kinetic energy still exists. This mechanism would account for scattered neutron energies in excess of those corresponding to a calculated equilibrium temperature of the nucleus. Such a definite, mechanical picture of the nucleus must,

however, be developed further with caution, and only insofar as additional experimental checks are available.

IV. THE NEUTRINO

Until about ten years ago it was generally believed that a nucleus was built up of protons, or groups of protons and negative electrons. The emission of beta-particles and of alpha-particles by naturally radioactive nuclei with energies greater than could be derived from the extra-nuclear structure was considered almost sufficient evidence of their presence there. But with the discovery of the neutron there came a change in point of view, which threw into strong relief the difficulties attending the assumption that electrons existed in the nucleus. These difficulties were concerned with such things as nuclear spin, nuclear magnetic moments, potential barriers, and the distribution in space of the electron matter waves. Protons and neutrons are now believed to make up the nucleus. What then of the negative electrons which are, without doubt, emitted by radioactive material? The modern view is that such disintegration electrons are created at the moment of their emission, just as a photon can be created and emitted by the extra-nuclear structure when a change of total energy occurs.

Thus some of the difficulties of the continuous beta-ray spectrum are solved, but not all of them. Here we are not concerned with the line spectrum of beta-rays, which arises through the action of nuclear gamma-rays on outer electrons. The beta-particles which appear to come from the nucleus have a wide energy spectrum, from zero to a definite upper limit, which is different for different members of a radioactive series. Thus there is a fixed change in the energy of the original nucleus, but a varying amount appears as energy of the beta-ray. In the face of the enormous mass of evidence which elsewhere supports the conservation laws of energy and of momentum, it seems unreasonable to throw them aside for this one case. Another solution of the difficulty is needed. Fermi, in 1934, assumed that another undetected particle, the neutrino, took part in the disintegration, carrying away a varying amount of energy so that the desired balance could be maintained.

In one sense this is a very logical solution, but since it puts the burden on something which cannot complain, it can hardly be called a satisfactory one; for the properties which the neutrino must possess to function as it is supposed to are nearly all negative—no mass, no charge, no magnetic moment, spin one-half. The problem is therefore to detect the neutrino to see if it carries away about the amount of energy expected.

The usual physical methods are useless, so that secondary effects must be used. Several attempts have been made to demonstrate the neutrino's existence by measuring the recoil momenta of other particles which take part in the disintegration process. Any unexpected momentum they possess must have come from the neutrino's recoil. The results of such experiments have not been entirely convincing, but, as the years pass, and data accumulate, the existence of the neutrino becomes more and more certain. A new investigation of this matter by Allen[13] is probably less clouded by ambiguitites of interpretation than any previous work.

To simplify the problem as much as possible, it is desirable to deal with a simple nuclear reaction. At least three entities must be involved, the nucleus, the beta-particle, and the neutrino. Therefore, to measure the momentum of the neutrino, it is necessary to measure the sum of the momenta of a nucleus and of a disintegration electron. The experimental technique would be simpler if the momentum of only one particle had to be observed. Kan Chang Wang[14] has pointed out that such a situation can be realized when a radioactive nucleus moves one step lower in the atomic sequence by absorbing a K electron into the nucleus. Be^7 is an unstable nucleus of this type, with a half-life of 43 days. If its decay is traced from counts registered by thin-walled Geiger-Müller tubes, it is found, by interposing suitable absorbing screens, that only gamma-rays are emitted, not accompanied by electrons. The reactions involving Be^7 appear to be

$$Be^7+e_k\rightarrow Li^7+\eta+1 \text{ Mev},$$
$$Be^7+e_k\rightarrow Li^{7*}+\eta+0.55 \text{ Mev},$$
$$Li^{7*}\rightarrow Li^7+h\nu+0.45 \text{ Mev},$$

though recent evidence from other studies suggests that the numerical parts of these equations may be in error by ten percent. In one case, an intermediate excited nucleus Li^{7*} is formed, but in any event, a neutrino, denoted by η is emitted. The detection of the neutrino therefore involves the observation of the Li^7 recoil nucleus. Allen impregnated a platinum foil with active Be^7, platinum being used on account of its high work function. By a preliminary heating, Be atoms were encouraged to diffuse to the surface of the foil, whence the resulting Li^7 atoms could recoil with as little energy loss as possible. Because of the relative values of the work functions, Li^7 atoms resulting from the disintegration of Be^7 were given off as positive ions, but other atoms evaporated in the neutral state. By virtue of their charge, the Li^7 ions were easy to handle. They emerged from the treated platinum foil with a range of velocities, depending upon the depth at which they originated.

Some of these recoiling nuclei were caught by the first electrode of an electron multiplier tube, which increased the current to such an extent that it could be handled readily with vacuum tubes. Such current was, of course, proportional to the number of Li^7 ions striking the first electrode of the multiplier. These ions, on their way to this electrode, were controlled by a retarding potential, and their number was measured as a function of the retarding potential until that potential was large enough to prevent any of them from being detected. In this way Allen found that the maximum energy of the recoiling Li^7 nuclei was about 45 electron volts. If there were no neutrino at all, then the energy of these nuclei would be that derived from the recoil of the gamma-ray of 0.45 Mev, or perhaps from the 1.0-Mev gamma-ray. The latter possibility was ruled out by the results of a supplementary experiment with coincidence counters which showed that no gamma-ray of this higher energy was observed at the instant when any Li^7 ion was being detected. The 0.45-Mev gamma-ray could give the recoiling nucleus only 15.6 electron volts of energy. This is so far below the figure of 45 electron volts found by Allen that it is safe to conclude that the difference (about 30 electron volts) was given to the recoiling nucleus by the neutrino.

Theoretical considerations show that the amount of excess energy, 30 electron volts, is only slightly dependent on the mass of the neutrino. The usual assumption is that the neutrino's mass is zero; but if it were as large as 0.2 of the electron's mass, the excess energy would be diminished by only one electron volt. In this respect Allen's experiment is inconclusive, but it has increased enormously the probability that the neutrino really exists.

V. COSMIC RAYS

It was remarked a year ago that a gratifying semblance of orderliness had been brought into the study of cosmic rays by the hypothesis that practically all of the primary incoming radiation consisted of fast moving particles, probably protons. Although this conception is definite and clear cut, yet there has not been time for it to make its mark in simplifying the interpretation of the behavior of cosmic rays subsequent to their entry into the atmosphere. The nature of the primary cosmic rays on the one hand and their behavior in passing through matter on the other, therefore remain as two distinct problems. A helpful summary of the processes which occur during the interaction of cosmic rays with matter has recently been given by Rossi and Greisen[15] in the *Reviews of Modern Physics*. They summarize the phenomena which occur in a qualitative way and also treat most of them mathematically. Some of these effects involve nuclear transformations; others do not involve nuclear change at all. The nuclear processes are comparatively rare and do not contribute significantly to those effects which are observed by counter trains, effects such as the absorption and scattering of mesotrons, and the production of showers by electrons and photons. The nonnuclear effects are of two kinds, collision processes and radiation processes. In the former of these the primary particle affects atomic electrons directly. The atom may be raised to an excited state, and slow-moving electrons may be ejected. In the latter, the primary particle is accelerated by the field of the nucleus and in doing so gives out radiation. For some particles one of these two effects predominates; for mesotrons and protons of moderate energy, for example, the

energy lost in passing through the atmosphere is due almost exclusively to collision processes.

Photons are emitted by charged particles only when they interact closely with the electric field of the nucleus. It may seem to be a step backward to state in 1942 that according to the classical electromagnetic theory a charged particle emits radiation whenever it undergoes acceleration, and to base on it parts of the theory of the passage of cosmic rays through matter. But it enables the role played by the controlling variables to be estimated in a qualitative way. For example, the radiation loss will be a rapidly increasing function of the atomic number because the acceleration which a particle experiences will depend on the charge of the nucleus. By the same token, the radiation loss suffered by electrons will be much larger than that of heavier particles like mesotrons or protons because the latter will not suffer nearly such severe accelerations in a nuclear field as will the lighter electrons.

The energy lost by radiation processes is carried away by photons having a spectrum of very wide limits, but in any one act a large percentage of the available energy is usually transformed. Hence, in strong contrast to the behavior of mesotrons and protons, whose energy is frittered away gradually, very fast electrons in passing through matter surrender only trivial amounts of their energy to low-energy processes, while changing a great deal into energetic quanta. These high energy quanta may now produce positive and negative pairs or else may produce new fast-moving electrons by Compton recoils. Thus a new supply of fast-moving light particles is created. The give-and-take continues; these fast-moving electrons again lose energy by radiation and the resulting photons again produce fast-moving particles. The whole process is summarized in the phrase "cascade shower." It is obvious from the description given that a shower may begin either with a high energy photon or a high energy electron.

It will be clear that if cosmic rays go through a very thin layer of material, the chance of a well-developed shower being formed is rather slight. On the other hand, if the rays enter extremely thick material, many of the showers which are produced will be absorbed in the material itself. There must exist a certain thickness of material, different, of course, for different materials, at which the showers are most fully developed. Transition curves, which show the growth of the ionization due to these showers, indicate that the thickness at which full development occurs is not quite the same for photons as for electrons. Since the penetrating ability of photons and of electrons is not the same, they will, in the first instance, begin to produce showers at different depths, but after the cascade process has been established there should be no essential difference in the transition curves for the two types of primary agent. Theory predicts that on the average, the photon-induced process should lag behind the electron-induced process by about the distance in which a photon has a twenty-five percent chance of being absorbed. The theory, which is quantitative, and which is much more specific than this qualitative statement implies, predicts the distance to be 0.3 cm in lead. Nereson[16] finds an experimental value very close to this figure.

The secondary processes accompanying the absorption of cosmic rays are very complicated. One method of attack on the problem is simply to find out with the help of suitable coincidence counters what different events occur simultaneously, with the presumption that such simultaneous events may be causally related. When simultaneous events have been recognized, then the conditions under which they are observed can be made increasingly stringent, and the number of variables controlling their appearance can be reduced to a reasonable number. Although no one experiment can be considered a crucial one, yet the data obtained from a well-chosen series may be expected, upon analysis, to indicate the key events which occur.

Along these general lines, Korff and Clarke,[17] in the high Rockies, have searched for a connection between the occurrence of showers and the production of neutrons. They find that coincidences between these events occur for showers generated in a variety of substances. The rate of production of neutrons is small, being of the order of 10^{-3} or 10^{-4} neutron per g per sec. at the summit of Mt. Evans, an altitude where cosmic rays are much more intense than at sea level.

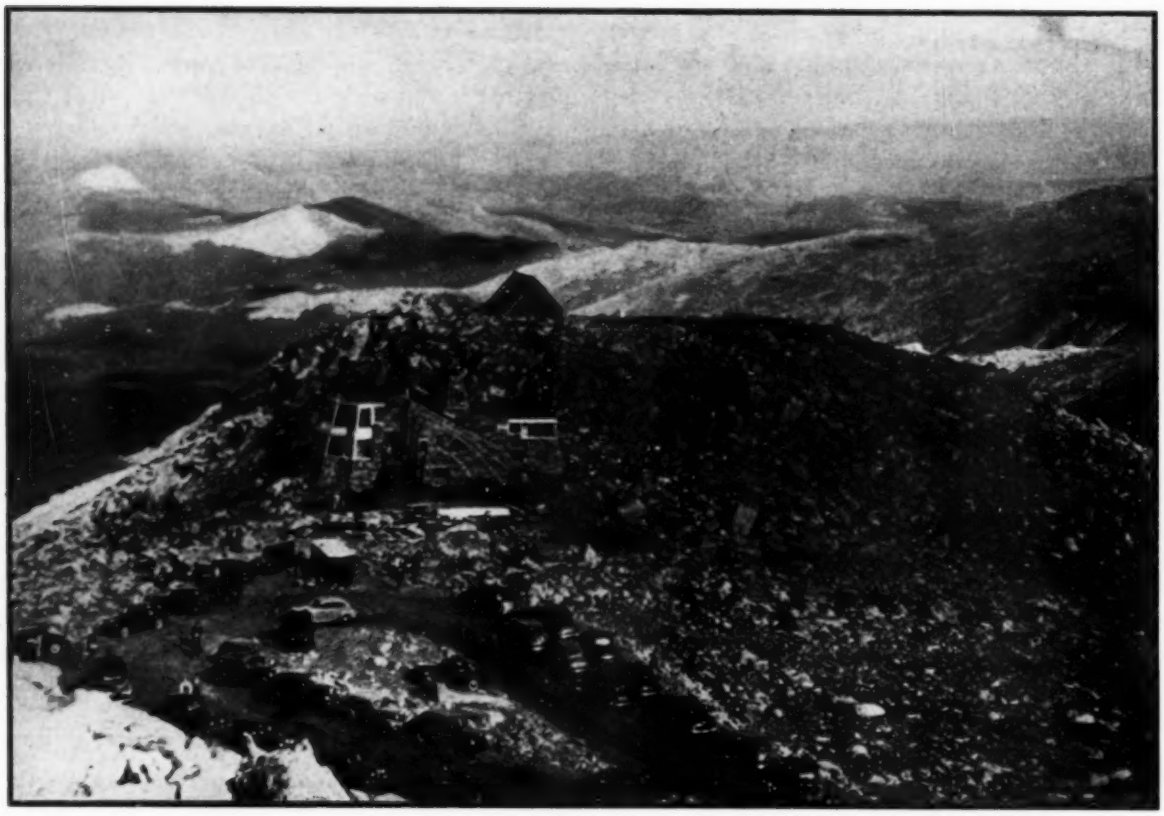

FIG. 3. View near the top of Mt. Evans, Colorado. The simple prismatic building is the cosmic-ray laboratory operated jointly by the University of Denver, the University of Chicago, and Massachusetts Institute of Technology. (Courtesy of S. A. Korff.)

The site of their experiments is shown in Fig. 3. In the middle distance is a hut which appears to be, and is, nearly all roof. This is the cosmic-ray laboratory maintained jointly by the University of Denver, the University of Chicago, and Massachusetts Institute of Technology.

In the same laboratory, Bostick[18] used a cloud chamber to study the non-electronic particles which accompany showers. He found heavy particles, which he interpreted as slow mesotrons or slow protons, in about 6 percent of his pictures; and in about 1 percent of the total expansions, there were pairs of penetrating particles, which must obviously have been produced nearby, and could not be primary particles coming from outer space or from the fringes of the earth's atmosphere. In closely related experiments, Auger[19] also found some low energy mesotrons accompanying the soft component.

The origin of the soft component of the rays is still a matter of debate. It is known to consist of electrons, which may arise from a variety of secondary processes, and may even include the last remnants of primary electrons, much slowed down by their journey through the atmosphere. Another possibility is that practically all the soft component can be accounted for by the electrons which are one of the decay products of mesotrons. This last hypothesis has been developed mathematically by Rossi and Greisen,[20] who were able to compare their theoretical results with the experimental values found by Greisen[21] for the intensity of the soft component as a function of altitude and of zenith angle. It will hardly surprise the reader to learn that the comparison led to the conclusion that there was something correct and something incorrect about each of the hypotheses. Rossi and Greisen summarize this phase of their work in the statement that electrons arising from the action of mesotrons, by decay or otherwise, should show a much less rapid variation of intensity, both with alti-

tude and with zenith angle, than is actually observed. The source of this fast-varying electronic component in soft cosmic rays is therefore probably to be found in secondary processes accompanying the absorption of fast primary electrons. At sea level, however, and also in the very high atmosphere, the numbers of electrons arising from mesotron decay appear to be nearly adequate to account for the whole intensity of the soft component.

The facts that mesotrons are produced in the high levels of the atmosphere, and decay on their subsequent downward flight have been among the most helpful basic concepts in the correct interpretation of cosmic-ray phenomena. Going one step farther, Auger and Daudin[22] have inquired whether or not other parts of the atmosphere may not also make contributions to the mesotron population. Their experiments showed that some particles emitted under thick layers of lead have the same penetrating power as low energy mesotrons. This result would indicate that at least some such particles are normally produced in air at low altitudes.

In a further search for quantitative data, Rossi[23] and his friends have continued their experiments to determine the lifetime of the mesotron. Since the lifetime of a mesotron varies with its momentum, being longer for energetic particles, it is necessary to specify its rest lifetime, as it were. Most values taken from the literature in the last two or three years run from one to three microseconds. In the recent experiments of Rossi, the value comes out at 2.8 ± 0.03 microseconds.

Turning now to the problem of the primary radiation, Millikan, Neher, and Pickering[24] have recently coordinated several results of a world-wide cosmic-ray survey (Figs. 4 and 5) to provide a working hypothesis concerning the distribution-in-energy of the rays as they enter the earth's atmosphere. They are very careful, however not to commit themselves as to the actual nature of the incoming radiation, beyond admitting that 60 percent of it may consist of charged particles, and it is to be regretted that they are yet unable to point out the features of their theory which are, and those which are not, in agreement with the proton hypothesis.

The general argument which these writers follow is this. They point out that all competent authorities agree that the only acceptable origin of stellar energy is the transformation of mass into other forms of energy, following the well-known Einstein relation $mc^2 = E$. Stellar energy is apparently adequately provided for by assuming, inside stars, the synthesis of simple atoms into more complex ones, but such a process does not give particle or photon energies as large as are observed in cosmic-ray experiments. It is therefore very satisfactory to know by direct observation that cosmic rays do not come from the stars but from a much more uniform distribution of sources throughout the nearby universe. Millikan, Neher, and Pickering assume that in interstellar space complete atomic annihilation is going on. The energy thus released is adequate to account for the observed cosmic-ray energy, and is much larger than that available from the synthesis of heavy atoms from simpler ones. The spectrum of the radiation thus generated in space will be governed by the total energies of the atoms which are most frequently found there, and here astrophysical evidence shows that the commonest atoms are hydrogen, helium, carbon, nitrogen, oxygen, and silicon. These occur in the approximate ratios 100, 10, 1, 1, 1, 1, respectively. Taking each of these atoms in turn, the three authors show that the magnetic fields of the sun and earth would debar radiation due to the annihilation of hydrogen from reaching the earth's surface, but that radiation from the other five annihilation processes would be able to reach the earth in certain localities. The less energetic rays will be able to reach low altitudes in the earth's atmosphere only at high magnetic latitudes, while the most energetic ones will penetrate to sea level at the geomagnetic equator. The five species of atoms, helium, carbon, oxygen, nitrogen, and silicon give rise to radiations of energy approximately 2 billion electron volts, 6 Bev, 7 Bev, 8 Bev, and 14 Bev, respectively. In proceeding northward or southward at a fixed altitude from the magnetic equator, the cosmic-ray intensity, due only to the 14-Bev component at the equator, will be enhanced by the appearance and detection of the less energetic components, each coming in at a fairly definite magnetic latitude. The 8-Bev radiation begins to be detected, for instance, at

a magnetic latitude of 33° or 34°, but is not found between this and the equator. Hence the over-all result is a series of steps or plateaus in the cosmic-ray intensity curve. The experimental evidence is not nearly as straightforward as these simple statements imply, but from an analysis of data from many parts of the world Millikan, Neher, and Pickering make out a fairly reasonable case for their hypothesis. The relative abundances of interstellar atoms should provide a check on the relative intensities of these five energy bands. At the moment, it is safe to say that the predicted energy in each band is not in contradiction to the observed energy, but quantitative estimates are still so rough that it is too early for a test of the whole hypothesis on this basis. What the general reader would welcome would be an interpretation of the findings of other schools of cosmic-ray research in terms of this five-band theory.

VI. X-RAYS

Considerable differences of opinion still exist concerning the diffuse reflections of x-rays from crystals. It will be remembered that a paper by Zachariasen[25] a few years ago revived an interest in the occurrence of faint spots in diffraction patterns obtained either by the Laue or the Bragg method. Since that time the pages of several journals have been enlivened by spirited discussions as to the real cause of these anomalous spots. A very extreme point of view is held by

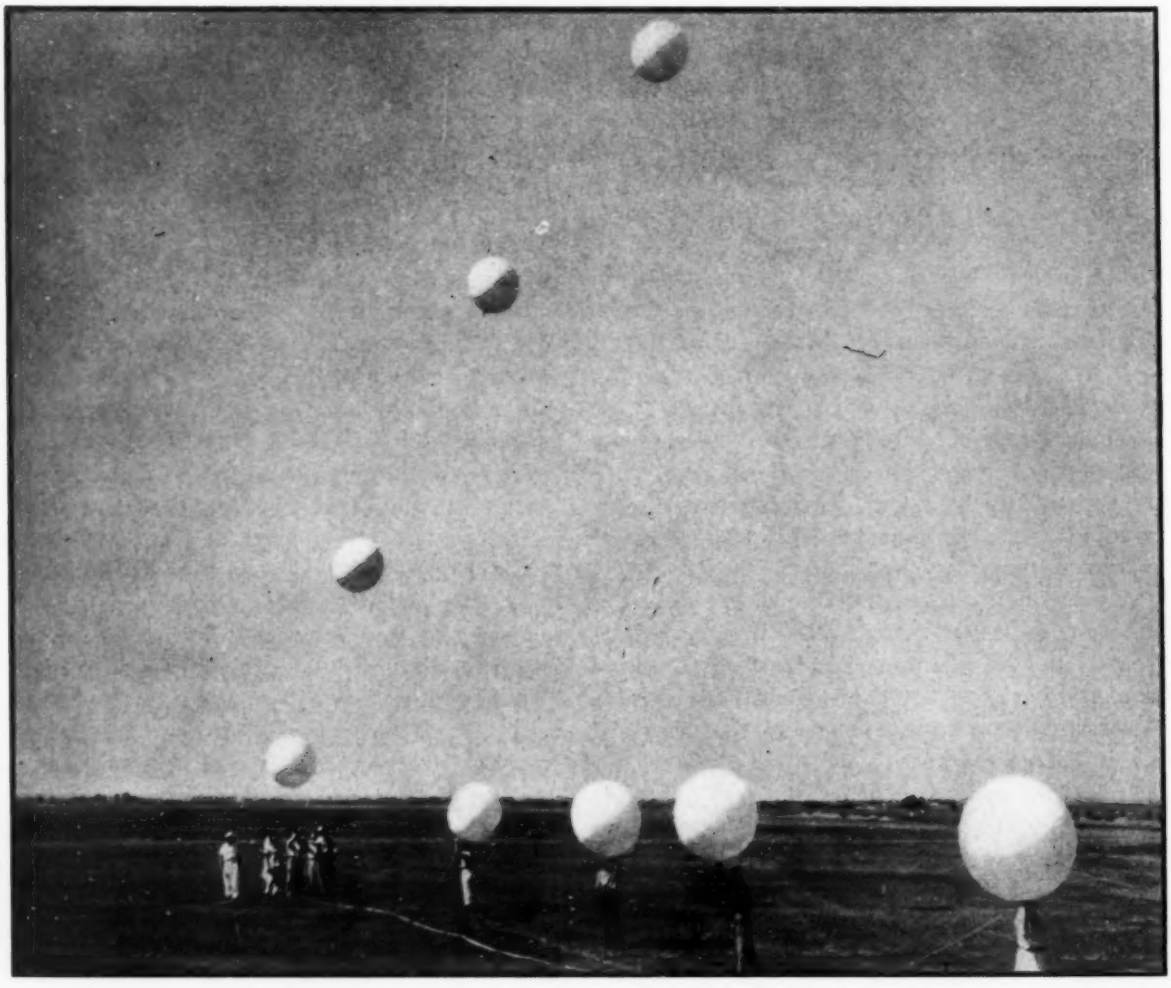

FIG. 4. Launching pilot balloons to carry an electroscope to near the limit of the atmosphere at Bismark, North Dakota. Readers who are not familiar with western states will find intersting extremes of terrain in Figs. 3 and 4. (Courtesy of R. A. Millikan.)

Raman and his school in India, which is at variance with views now current in Great Britain and the United States of America. A clear summary of the situation has been given by Preston,[26] who is quoted directly in the following account. The progress made in the investigation of this interesting subject in India has recently been reported in the *Proceedings of the Indian Academy of Science* of October, 1941, which is wholly devoted to a "Symposium of Papers on the Quantum Theory of X-Ray Reflection and the Raman Reflection of X-Rays in Crystals." This description of the subject matter reflects very clearly the difference in the interpretation of the phenomena which exists between French, American, and British physicists on one hand, and the group of Indian physicists at Bangalore working under the leadership of Sir C. V. Raman on the other.

When a single crystal of, say, aluminum, rocksalt, or sylvine is mounted in a beam of x-rays which traverse the crystal in a direction parallel to a cubic axis, a Laue photograph is obtained if the beam consists of white radiation. In addition to the Laue spots, there appears on well-exposed plates a number of streaks, running through the Laue spots, which apparently should have no business there. When the composite x-ray beam is replaced by a monochromatic beam, the usual theory of crystal diffraction tells us that no reflection should be observed unless the crystal is oriented in a particular way. In general, the condition for reflection will not be satisfied, except by a lucky accident, and a blank photograph should result. However, in fact, reflections are observed. They are faint, but have the symmetry proper to the crystal axis in which the incident x-ray beam lies. It is this background of non-Laue diffuse reflections that is attracting the attention of x-ray crystallographers. To what is it due?

There appear to be several possible answers to this question. The most comprehensive is perhaps to say that the diffuse background arises as a direct result of departures from geometrical perfection in the crystal architecture. A periodic flaw, a regular precipitation of an impurity, and the temperature vibrations of the atoms are all possible and probable causes. It is the task of the experimenter to devise means of identifying

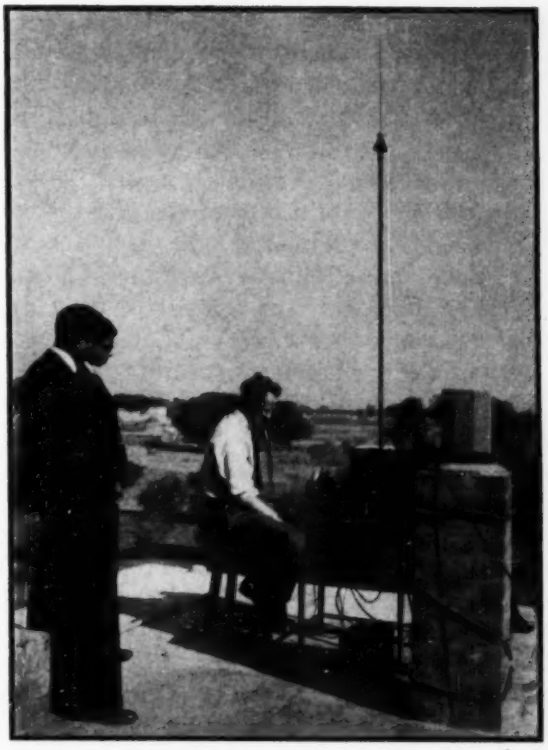

FIG. 5. Two young Indian gentlemen watch while W. H. Pickering receives cosmic-ray signals coming from a transmitter high in the atmosphere. The scene is the top of a building at Agra, India. (Courtesy of R. A. Millikan.)

the different causes so that use may be made of the machinery provided by the mathematician to enlarge our knowledge of the solid state. Those features of the background reflections which occur in crystals of pure substances, so that flaws and chemical segregation are excluded from consideration, are evidently of great importance. There is general agreement on all sides that this background is due to movement of the atoms or molecules of the crystal from the positions of perfect geometrical alignment. The differences of interpretation arise in assigning the cause of the movement, and in the mechanism of x-ray scattering. In Great Britain and the United States, the whole effect is ascribed to the static geometry of the crystal, so the diffuse background is a picture of the dynamic vibrations of the crystal. The undisturbed crystal can be regarded as a medium in which the density varies periodically in space, and the effect of the temperature vibrations is to superimpose a spectrum of much longer elastic waves on the natural periodicity of

the crystal. The whole crystal then diffracts as a unit, and the resulting pattern consists of the usual Laue reflections plus a background due to the motion of the atoms.

The point of view adopted by the Bangalore group of physicists is rather different. To begin with, the quantum aspect of the interaction of x-rays with the atoms of the crystal is emphasized. The radiation scattered from an oscillating atom is stated to consist of three components the amplitudes of which depend on the amplitude of oscillation of the atom, and which differ in frequency. The first component, which gives rise to the normal reflections, has the frequency ν of the primary x-ray beam, while the other two have frequencies $\nu \pm \nu'$, where ν' is the frequency of atomic oscillation. The frequency change is unfortunately too small to be measured directly. This description of the mode of formation of the anomalous spots can be shown to lead to certain contradictions. For example, it can be used to show that the diffuse spots must be in part controlled by the elastic properties of the crystal; but such a dependence is essentially denied by Raman's primary assumptions.

Preston concludes, perhaps with undue caution, by saying that the quantum hypothesis as set out by Raman is unlikely to be reconciled with the elastic wave explanation unless one or the other hypothesis is radically altered; and that it must be admitted, at all events, that the thermal-elastic theory gives a reasonably accurate account of the observed facts. On the other hand, Lonsdale,[27] who, jointly with Smith, is responsible for the majority of the experimental work on this subject in England, is a much bolder champion of the "classical" theory than others. She calls attention to some inaccuracies in experiment, and to some errors in interpretation which affect the conclusions of Raman and his colleagues, and emphasizes the validity of the classical interpretation of the Indian work.

The real importance of the anomalous x-ray spots is not, however, in this argument about their origin but in the use to which they may be put to help in the solution of other problems. As Lonsdale hinted nearly two years ago, the diffuse spots are very closely bound up with the elastic properties of the crystal. The original theory of Waller has been interpreted and applied by Jahn[28] in such a way as to relate the appearance and size of the spots to the elastic constants of the crystal. In general, the more inelastic the crystal, the bigger and fuzzier the spots are. The pattern for tungsten, for example, which is highly elastic, is much tidier and less intense than that for sodium or lead.[29] The diffuse spots of tungsten, indeed, appear to be only one-thirtieth as strong as those of sodium; while those for lead are half as intense as those of sodium. These values are in agreement with estimates made from Jahn's calculations. This is by far the most important result which has emerged from these studies to date, and it promises to be of very great practical importance in the future. It will allow elastic constants to be determined without straining the crystal.

VII. ACTIVE NITROGEN

There is a fascination about active nitrogen which brings its devotees back after years of absence. First discovered in 1900, the main features of its behavior are well known, but in the detailed explanations which have been offered for these there were many contradictions. The customary mode of excitation is by a high frequency electrodeless discharge. Under its influence the nitrogen glows with a yellowish light, which, under the proper conditions, remains visible for several hours after the discharge ceases.

Lord Rayleigh[30] has recently published a new series of papers on the subject, which provide some definite facts to be taken into account in any theoretical explanation of the phenomenon. In the first place he has, by means of a simple photometer, measured the luminosity of a known quantity of active nitrogen at intervals of a few seconds during its initial rapid decay; and from the data has arrived at the integrated light emitted per cm^3 of nitrogen under the most favorable conditions. This turns out to be 3.18 candle-sec. per cm^3 under standard temperature and pressure. Thence, knowing approximately the average wave-length of the emitted light, it is possible to calculate how many quanta are emitted per molecule of nitrogen under the conditions of the experiment. The answer is 1.3×10^{-3}.

If active nitrogen be compressed, its brightness increases, and vice versa. Raleigh finds that if the gas be handled in a simple manner as in a pump, the brightness varies inversely as the cube of the volume. This result is in agreement with two other series of experiments. In one of them, additional ordinary nitrogen was admitted to a bulb containing the glowing gas, increasing the pressure about fivefold. The increase in brightness was very closely of the same order of magnitude, so that the brightness is proportional to the concentration of inert nitrogen, because here the concentration of active nitrogen remained fixed. In the other series, two bulbs containing nitrogen at equal pressures were connected by a stopcock. First, the gas in one was activated. Upon opening the stopcock, the active component diffused throughout the double volume of inert gas, reducing the active concentration to one-half of its original value. The intensity of the light was found to drop to one-fourth of its original intensity. Hence the luminosity is proportional to the square of the concentration of active nitrogen. Therefore, in a simple "pump" experiment, wherein the concentrations of the active and inert gas must be increased together, the luminosity would be expected to vary as the cube of the concentration, in agreement with the result quoted above. A difficulty was found here, however, for upon allowing partially active nitrogen to expand into a vacuum, so that both concentrations were diminished by the same factor, the cube law was found to be a somewhat inaccurate prophet of the intensity.

Rayleigh noticed that pieces of sheet gold, silver, copper, or platinum could be made red hot or even melted by immersion in active nitrogen, and he used this property to make an estimate of the amount of energy which must be abstracted from the gas in the process. The results are startling. In a "continuous flow" experiment, in which the active gas passed in a stream from the site of the discharge to another bulb containing the small sheet of metal, it was found that the power radiated by the hot metal was such that it was necessary to assume that *every* molecule which passed through the discharge carried some 5 or 10 electron volts to the metal foil. This might conceivably be interpreted as implying that the energy is carried by dissociated atoms which associate again to N_2 at the surface of the foil, but only on the assumption that every molecule was dissociated. At first sight this seems so unlikely that it might be ruled out of consideration. It would follow that the luminous energy radiated as the familiar afterglow, under favorable conditions, represents only a tiny fraction of the total energy transported by the gas to the metal.

The addition of a little oxygen to glowing nitrogen has an important effect on the intensity. In one case it was increased 32-fold. Rayleigh shows that this must be a wall effect. The logical thing to do, then, is to experiment with various treatments of the walls. As found by Herzberg, strong preliminary heating in vacuum diminishes the subsequent afterglow. It is now found that heating in nitrogen at atmospheric pressure does the same. Heating in oxygen, even at 1-mm pressure, restores the container to its original helpful state. It seems clear that these effects cannot be explained easily by the formation or removal of surface layers of gas. The behavior of the glass surface is therefore complex. The behavior of the gas itself away from the wall is of more fundamental interest. By studying the glow at the center of a large flask, it was shown that the best results were obtained with very pure nitrogen, and that the addition of a trace of oxygen had no favorable effect in promoting the active nitrogen phenomena.

Nearly all these details of behavior now receive an explanation in a paper by Debeau,[31] who learned by repeating an old observation of J. J. Thomson's that nitrogen is practically completely dissociated in the electrodeless discharge. Once this is established, it is possible to construct a very definite picture of the process of formation and decay. After the dissociation, according to Debeau, the first stage is the formation of a "collision complex," which may then react with another molecule to form nitrogen in the $B^3\Pi$ excited state with 9.84 electron volts of energy, which subsequently degenerates into the $A^3\Sigma$ metastable state with emission of afterglow radiation. Alternatively, the collision complex may descend directly to the $^1\Sigma$ state, the ground state of the nitrogen molecule, with liberation of energy as in Rayleigh's experiments on the heating of metal foils. This latter is much the

more probable course of events, so that the heating phenomenon is a parallel and independent rather than a previous or subsequent step in the life of active nitrogen.

VIII. GENERAL TRENDS

The physics journals of this country grow slimmer and slimmer as an increasing number of her scientists turn from academic problems to investigations of military, naval, and aeronautical importance, the results of which cannot be broadcast to the world. Very few reports on entirely new topics are being published, and most recent papers, like those summarized in this article, are concerned with gathering up the loose ends of research programs initiated several years ago. Publications in the field of applied physics, such as appear monthly in this journal, are frequently devoted to general topics viewed from different angles. An experimental observation, being a matter of fact, need not be of recent date to be interesting. What makes it interesting is the light in which it is viewed, and here it often happens that modern theories from exceedingly diverse branches of physics can be trained on a single problem. For this reason the various reports of conferences which are published from time to time take on an added importance for industrial work. These trends of the professional journals will undoubtedly be accentuated in the immediate future, and as time goes on, the need will grow greater for that peculiar type of intuition which is able to see the significant cross-relations between what may be superficially unrelated topics.

In a year when physicists have little time to spare, the writer is grateful for the cooperation of those men who have lent him photographs to illustrate this article. He is also deeply in the debt of the authors of those papers which he has read recently, and from which he has quoted freely, often without specific acknowledgment. Finally, thanks are due to his colleagues, especially C. D. Hause and J. W. McGrath, who have read the manuscript and have given him many helpful suggestions.

BIBLIOGRAPHY

(1) N. F. Mott and R. W. Gurney, *Electronic Processes in Ionic Crystals* (Oxford University Press, 1940).
(2) F. Seitz, *The Modern Theory of Solids* (McGraw-Hill Book Company, 1940).
(3) A simple account is given by J. M. Kendall, Nature **150**, 136 (1942).
(4) R. C. Jones, Phys. Rev. **58**, 111 (1940), and other references quoted there.
(5) S. P. Frankel, Phys. Rev. **57**, 661 (1940).
(6) K. E. Grew, Nature **150**, 320 (1942).
(7) G. L. Ragan, W. R. Kanne, and R. F. Taschek, Phys. Rev. **60**, 628 (1941).
(8) G. Breit, H. M. Thaxton, and L. Eisenbud, Phys. Rev. **55**, 1108 (1939).
(9) H. Carroll, Phys. Rev. **60**, 702 (1941).
(10) H. Tatel, Phys. Rev. **61**, 450 (1942).
(11) W. Rarita and J. Schwinger, Phys. Rev. **59**, 556 (1941).
(12) H. F. Dunlap and R. N. Little, Phys. Rev. **60**, 693 (1941).
(13) J. S. Allen, Phys. Rev. **61**, 692 (1942).
(14) Kan Chang Wang, Phys. Rev. **61**, 97 (1942).
(15) B. Rossi and K. Greisen, Rev. Mod. Phys. **13**, 240 (1941).
(16) N. Nereson, Phys. Rev. **61**, 111 (1942).
(17) S. A. Korff and E. T. Clarke, Phys. Rev. **61**, 422 (1942).
(18) W. H. Bostick, Phys. Rev. **61**, 557 (1942).
(19) P. V. Auger, Phys. Rev. **61**, 684 (1942).
(20) B. Rossi and K. Greisen, Phys. Rev. **61**, 121 (1942).
(21) K. Greisen, Phys. Rev. **61**, 212 (1942).
(22) P. Auger and J. Daudin, Phys. Rev. **61**, 549 (1942).
(23) B. Rossi, K. Greisen, J. C. Stearns, D. K. Froman, and P. G. Koontz, Phys. Rev. **61**, 675 (1942).
(24) R. A. Millikan, H. V. Neher, and W. H. Pickering, Phys. Rev. **61**, 397 (1942).
(25) W. H. Zachariasen, Phys. Rev. **57**, 597 (1940).
(26) G. D. Preston, Nature **149**, 373 (1942).
(27) K. Lonsdale, Nature **149**, 698 (1942).
(28) H. A. Jahn, Proc. Roy. Soc. **A179**, 320 (1942).
(29) K. Lonsdale and H. Smith, Nature **149**, 21 (1942).
(30) Rayleigh, Proc. Roy. Soc. **A180**, 123 (1942).
(31) D. E. Debeau, Phys. Rev. **61**, 668 (1942).

Electrostatic Electron Microscopy. II[1]

BY C. H. BACHMAN AND SIMON RAMO

Electronics Laboratory, General Electric Company, Schenectady, New York

This paper is a continuation of the description of problems arising in the development and design of an electrostatic electron microscope. The present article discusses depth of focus, lens and field stops, shielding, manufacturing tolerances, the choice of the number of stages of magnification, and alternative methods of viewing and recording the final image. A following paper will describe a completed instrument.

DEPTH OF FOCUS

THE depth of focus of any electron-optical system, whether magnetic or electrostatic, may be computed in the same way as it is computed for ordinary light-optical systems. Having chosen a minimum resolution, it is necessary only to examine the paths of extreme rays to or from the object or image as a function of the departure of either from best focus position. Accordingly, the theory will not be further considered here. The electrostatic microscope, having common accelerating and lens potentials, is one in which the focal length of the lenses is fixed by their geometrical form and dimensions, and which, for all practical purposes, is completely independent of the voltage applied to the instrument. Focusing is thus most conveniently done in the same way as in an ordinary light microscope—namely, by the axial motion of one or more parts of the system. Simple depth of focus considerations show that it will not prove practical to focus by moving the fluorescent screen (or photographic plate); though the magnification change will be large, the correction effect to neutralize the specimen departure from best location will be very small. This scheme, if useful in focusing at all, would be so only as a very sensitive micrometer method. It follows conversely that one cannot appreciably alter magnifications by moving the specimen without losing resolution quickly. Thus, the best plan is to obtain sharp focus by axial motion of the specimen or some electrode in the electron-optical system near the specimen.

LENS AND FIELD STOPS

In an electrostatic unipotential lens, the lens stop cannot be placed at the center of the lens. It becomes necessary then to consider the relative effectiveness of various possible locations for the limiting apertures. Small apertures already exist at the entrance and exit of the lens, and in general others may be placed ahead or beyond the lens region. Every electrode in the optical system that allows some electrons to pass through it and rejects others which have too great a departure from the axis, acts partially as a field limiter and partially as an aberration limiter.

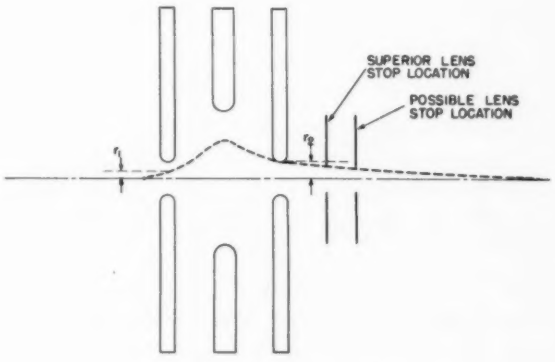

FIG. 1. Lens stop locations.

Suppose, for example, that it is desired to limit the spherical aberration of the objective lens. The electrons are assumed to originate at a point on the axis very near a focal point and to cross the axis again at some distance from the lens (Fig. 1). The electron trajectory for lens potential distributions previously discussed[1] is approximately as indicated in Fig. 1. Electrons which enter the lens region with a displacement r_1 leave the lens with a much larger displacement r_2. Approximate computations for the case of voltage drops in the lens of about one-half anode-cathode voltage indicate that r_2/r_1 may easily be as great as five and usually would be

expected to be greater than two. Accordingly, in the interests of stopping the lens without having to resort to minute aperture diameters (whose rough edges may bring in field emission and image distortions), it would be best to regard the region beyond the lens exit as the best lens stop location.

The stop should be placed as close as possible to the exit since, as indicated in Fig. 1, the farther away the aperture is placed, the smaller it must be. Furthermore, it should be evident that as the stop approaches the image plane, it commences more and more to be a field limiter rather than a lens aberration limiter.

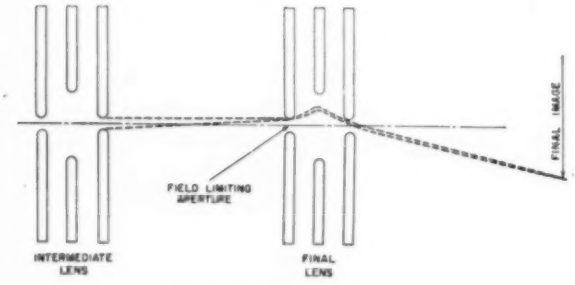

FIG. 2. Field stop location.

If possible, it is advisable to limit the rays entering the lens to as small a bundle as is conveniently accomplished by a well-rounded aperture—consistent, of course, with the ratio of r_1 to r_2. This procedure will lessen the possibility of secondary electron production on the lens side of the exit aperture. These secondaries, caused by unwanted non-axial electrons, return into the lens region where they bombard the electrode surfaces and the insulation.

To consider the location of the stops which limit the field, we must move to the last lens of the system. For this lens we may in most cases consider that the electrons arrive with very small angles of inclination to the axis since they will be coming from a rather small opening at the exit of the previous lens which is relatively far away (Fig. 2). If the lens is so designed that the focal points are near the entrance and exit of the lens, then an initially, nearly parallel ray will, of course, be found to cross the axis rather close to the exit plane (Fig. 2). Thus the exit aperture of the last lens may be smaller than the entrance aperture before it begins to limit the field.

To summarize, the exit of the objective lens limits the aberrations of the system while the entrance of the last lens limits the field whenever the entrance and exit apertures of each lens are of equal diameters.

SHIELDING

The electron beam, from the source to the screen or photographic plate, must be shielded both from stray electrostatic and stray electromagnetic effects. The electron gun itself must not be overlooked since, if the shielding problem is well taken care of there, it becomes possible to design the gun so that it may be permanently aligned with the remainder of the electron-optical system in manufacture and will not require re-alignment by the operator even when the filament is changed.

Electrostatic shielding is easily taken care of in the gun by the use of shielding cylinders (Fig. 3), every part of the instrument being at ground potential but the cathode and the interior portions of the focusing lenses. The authors have developed a lens assembly which is exceedingly compact and which uses a single rod inside the vacuum envelope to connect the negative potential electrodes of the lenses to the cathode. The stray electrostatic field of this connector may again be shielded from the beam in the region between lenses by the use of further cylindrical shields (Fig. 3). However, inside the lens itself, the center electrode is energized asymmetrically by it, so it becomes necessary to choose the distance of the connector to the axis to be large compared to the spacing between lens electrodes. The detrimental effect due to this source can be detected in the image resolution since it will vary with azimuthal angle about the axis. This disturbing effect in the symmetry of the electric field of the lenses constitutes one limit to the reduction in diameter of the microscope body for any given lens design.

There are two classes of magnetic shielding problems. The field due to the gun's filament current must be attenuated highly before it reaches the region of the specimen. The entire electron path must, in addition, be shielded from external magnetic fields. The former problem is, of course, simplified if high frequency is used for heating of the filament. For the use of low fre-

quencies, such as 60 cycles, shielding has been obtained by adding sufficient mu metal in the gun components (Fig. 3) so that the magnetic field of the filament can reach the specimen only through the small vacuum pumping holes or the holes that must exist in the gun anode and defining apertures.

By arranging the microscope to be of minimum diameter and by using a multiple lens imaging system it is possible to reduce the over-all size of the entire instrument so that one single magnetic shield may enclose the entire structure for general shielding from external magnetic effects. The amplitude a transverse a.c. stray magnetic field may be permitted to reach before interfering with resolving power down to below 100A has been computed to be of the order of 10^{-6} gauss, averaged over the electron beam's length.[2] For a given length of path and electron velocity, the resolution (as limited by a stray a.c. field) will increase with the magnification; this, because the ultimate deflection of the electrons at the image is divided by the magnification to obtain resolution referred to the object plane. With everything else fixed, the resolution will vary inversely with electron velocity (or the square root of anode-cathode voltage).

The chief difficulty in predesigning a suitable magnetic shield for an electron microscope is that the permeability of the shielding material is not known in the range of the exceedingly small field strength to which the inner layers of the shielding will be subjected. One has no better choice then than to try experimentally various amounts of turns of a given thickness of shielding until the required amont of shielding is obtained. Possibly the electron microscope itself will serve eventually as a means for obtaining such data.

The first-order effect of a d.c. field is to deflect the whole image bodily. If there were truly no relative motion of the various electron beams which yield the image, resolution would be unaffected; the only effect would be a disturbance in the alignment of the system. Such a condition would call for absolute constancy of the disturbing field and the electron velocity. Now, quite apart from resolving power, to keep a 25,000- to 50,000-volt electron beam centered, say within one-hundredth of a centimeter over a distance of the order of 50 centimeters, requires that the transverse d.c. field be no higher than about 10^{-3} gauss. Obviously this degree of refinement in centering the beam along the axis may be relaxed with distance from the objective lens since the later lenses can tolerate greater departure of the beam from the axis. This factor is important in designing an instrument which is permanently aligned in manufacture. Magnetic shielding sufficient to protect the beam from transverse a.c. stray fields will at the same time protect against this disturbance in alignment due to stray d.c. fields of somewhat greater strength. If the a.c. 60-cycle and d.c. fields are of comparable strength and the a.c. fields have been sufficiently well attenuated by shielding, then a generous ripple in the voltage supply may be permitted before there is a limiting of resolution by the d.c. field.

The foregoing statements apply to all electron microscopes. An additional factor which comes up in the electrostatic instrument is that in the central region of the lens the electrons are traveling at reduced velocity and thus are more susceptible to deflection. The most serious effect here is that electrons on the axis are slowed down less than electrons at the beam edge, since the potential varies over the lens cross section. This is another way, in other words, in which even a d.c. transverse magnetic field would work to destroy resolution because electrons at different distances from the axis will receive different deflections from the same strength of stray field. It is possible to estimate the difference in deflection of electrons passing through the lens on the

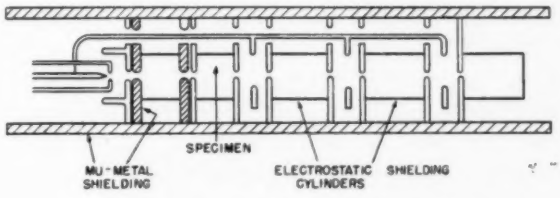

FIG. 3. Shielding of electrostatic microscope.

axis and a few mils away from the axis by the aid of approximate potential distribution functions. For lenses in which the lens drop[1] does not exceed one-half of the anode-cathode voltage, this effect will not limit the resolution if the shielding is already adequate from the standpoint of alignment accuracy. In a design, however, which seeks to use a very high voltage drop at

the center of the lens compared to the cathode-anode voltage, the effect must not be overlooked.

A stray magnetic field that is axial, since it acts symmetrically, may be regarded as an additional electron lens which, if it failed to pulsate at all in focal length, would not be at all objectionable. An a.c. magnetic field or even a d.c. magnetic field along the axis may prove troublesome in this respect for the desired simple electrostatic microscope in which an appreciably greater voltage ripple might otherwise be allowed. It is possible to compute the order of magnitude of this effect for a given magnetic field strength by simply adding to the focusing action of the electrostatic lens system a small oscillating magnetic lens whose focal length may be related to the magnetic field strength from the simple theory of magnetic lenses. Such a simple analysis leads to the conclusion that if the shielding is adequate to protect the electron path against transverse fields and it is allowed to protrude beyond the electron path an amount equal approximately to the radius of the shielding tube, the axial magnetic field will die off rapidly enough so that there will be insufficient strength at the specimen to affect the resolving power. This statement assumes that the axial field is of magnitude comparable to the cross magnetic field. Particularly strong axial fields should probably best be regarded as an unfortunate choice of location for the instrument and remedied in a manner more straightforward than the addition of axial shields.

MANUFACTURING TOLERANCES

Glass lenses used in high-grade light optical instruments are known to require the most exacting precision in manufacture. Fortunately, the electrons in electron optical lenses do not cross electrode surfaces, but only equipotential surfaces whose forms are indirectly determined by the adjacent conductors and impossible tolerances are not called for in order to produce higher than light microscope resolving power. One approach to the precision manufacturing problem is simply to have every part of the microscope made with as high a precision as possible. Such a criterion is not very practical, however, for commercial production. Here it is desirable, if not essential, to know where the high tolerances may be relaxed and to what precision one must necessarily build certain parts of the instrument. Naturally, it is difficult to obtain very precise specifications at this stage of the art. However, it is possible to obtain some idea of the orders of magnitude of permissible distortions by a few simple attacks. These methods and chief results will next be described.

A complete electrostatic lens may be thought of as consisting of many thin lenses in series. Misalignment of any one of the lens electrodes (so that the three electrodes do not have a common axis) may be thought of as a misalignment of some of the thin lenses which are mainly in the immediate vicinity of that misaligned electrode. The electron beam when passing through these thin lenses will appear to these misaligned lenses as a non-axial beam. Aberrations will result which can be computed as due to the failure of all electrons to be completely axial. With such information as has been described previously[1] as to the size of aberrations for a given electron path departure from the axis, and with some approximate distribution of the lens action among the regions near the various electrodes, the order of magnitude of this effect may be estimated.

Another type of aberration might be caused by placing even perfectly formed electrodes in planes which are not all parallel to each other; or in other words, not perpendicular to the axis. Here one can think of such a lens as consisting of many lens sections in parallel (Fig. 4) around the axis so that with electrode spacing differing around the axis the focal lengths of these elements will differ accordingly. Now the variation of focal length that can be permitted in a lens, i.e., the tolerable spread of focal length that will just allow the desired resolution has been previously

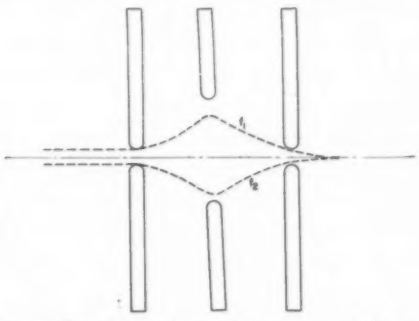

FIG. 4. Focal length variation around the axis.

computed.[1] Also approximate relations between focal length and the various inter-electrode spacings are known. From such information one can estimate the focal length spread and consequently the resolution limit due to the variation of inter-electrode spacing with azimuthal angle around the axis.

A third manifestation of insufficiently close manufacturing tolerances is the lack of concentricity of any one electrode. For example, a hole in the central electrode may not be a perfect circle. This is similar to the two preceding distortions, especially the case of variation of focal length with angle around the axis due to non-parallel lens elements. The difference, however, is that in the case of lack of concentricity, one may expect an averaging effect. If, say, one part of what should be a circle protrudes toward the axis slightly, then the rest of the circle tends to shield and diminish the effect of that single disturbance (Fig. 5a). Though this particular case has not been examined theoretically, closely related cases have been treated. Figure 5b shows the case of a hemispherical hub on one of two parallel plate conductors. This case has been worked out[3] and it is shown that the disturbing effect of the hub dies off very rapidly with distance from the plane—rapidly, that is as compared to the case of a spherical hub alone (without the benefit of the "averaging out" or shielding of the plane). From such analyses, one may make a reasonable guess as to the averaging factor to be expected when small distortions occur on the face of electrodes. The remainder of the estimation of the effect on resolution is as in the previous example.

The results of these rough analyses indicated first of all that only the objective lens needs to be given careful attention, since the magnification which is usually designed into this stage sufficiently reduces the tolerances required for the second and third stages so that there should be no problem in manufacture. As to the objective lens, approximate computations called for tolerances of a little better than one-thousandth of an inch in axial alignment, concentricity of individual electrodes, and inter-electrode spacing variation around the axis in order that resolving powers superior to 100A be possible.

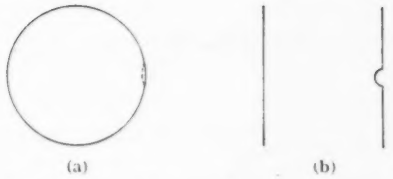

FIG. 5. Electrodes with imperfections in manufacture.

Since these computations are admittedly of questionable accuracy, it appears excusable at this time to attempt to manufacture the objective lens with tolerances considerably better than one mil or the tolerances may well be expected to set the limit to resolution.

CHOICE OF THE NUMBER OF STAGES OF MAGNIFICATION

In an electrostatic microscope having disk-type electrodes, all capable of fitting into one cylindrical enclosure, it becomes inviting to consider radically shortening the electron microscope structure by the use of more than two stages of magnification. This shortening of the structure, in addition to the obvious advantages in vacuum pumping operations and the saving of material and over-all weight, yields a system which is much more easily shielded and aligned.

It is well worth knowing beforehand, however, whether or not the choice of the number of stages and the spacing between lenses will materially affect the resolving power, the brightness of the final image for a given current density at the specimen, and other over-all performance and design characteristics. Let us reconsider then the various design conditions that have been previously discussed to determine how these matters will depend upon the number of lenses.

Expressions were derived in the previous paper[1] for resolution as limited respectively by spherical and chromatic aberrations:

$$\delta_{\text{spher}} = (pS/2f^3)r^3; \tag{1}$$

$$\delta_{\text{chrom}} = (p/f)(\Delta V/V)r. \tag{2}$$

S is a characteristic constant of the lens type, f is the lens focal length, r is the radius of the lens stop (evaluated at the lens exit), p is the object distance, and ΔV and V are electron voltage spread and average voltage, respectively. When the number of stages is varied for a fixed f and fixed over-all magnification, the magni-

fication per stage and the object distance p will also vary. With an increase in the number of stages, p increases.

Since the resolution as limited by spherical aberration [Eq. (1)] varies with the cube of the stop radius, a small percentage change in the latter will make up for a larger change in p. We can assume, therefore, that only a negligible decrease in lens stop need be made if the number of stages is increased say from two to three or four, if the resolution is to be held constant.

TABLE I.

No of Stages	p (cm)
1	1.00
2	1.01
3	1.05
4	1.10
5	1.15

If the resolution is limited by chromatic aberration [Eq. (2)], then the stop radius must be reduced in the same proportion as p is increased to hold constant resolution. Table I gives the variation in p with number of stages for a fixed over-all magnification of 10,000× and a fixed focal length for all stages of one centimeter.

When taking account only of spherical and chromatic aberrations, there is little need for considering any but the first stage. Regardless of what number of stages is selected, the magnification per stage will always be greater than unity, so that the angle of rays entering the second lens coming originally from an axial point on the specimen or its image will be less than that entering the first lens. Also the object for the second lens need not be imaged with so good a resolving power (referred of course to the second lens magnification scale).

Let us consider next the brightness of the final image for a given electron density passing through the specimen as a function of the number of stages. A limit in one direction may be obtained by assuming that each point of the object appears as a source of electrons spread uniformly over an angle of 2π solid radians (Fig. 6). The brightness is then determined by the opening solid angle θ of the objective lens. For a given stop diameter θ is seen to decrease according to $1/p^2$. If the diameter of the aperture is decreased to preserve resolution as the number of stages is increased, then the brightness is further decreased. When chromatic aberration is the limit to resolution (a case much more pessimistic as regards brightness than if spherical aberration is assumed as the limit), the brightness would decrease with the fourth power of object distance. Thus a two-stage instrument will have around 16 percent more intensity in the image than a three-stage instrument for constant focal length lenses, constant over-all magnification, and constant resolution as limited by chromatic aberration.

For a wide range of specimens, it certainly will not be true always that the opening angle determines the brightness as assumed in the previous pessimistic reasoning. The true situation on the average will probably be somewhere between the above assumption that each point of the object is a source, and the following picture: The specimen is generally transparent and thus allows electrons to pass through practically undisturbed in angle of inclination to the axis, which angle is set by the gun to be small regardless of the number of stages. The denser portions of the sample deflect or absorb electrons and produce correspondingly less brilliant spots on the final screen. With the assumption that the gun sends electrons through the specimen at an angle that is smaller than the opening angle of the objective lens, the brightness is hardly then dependent upon the number of stages.

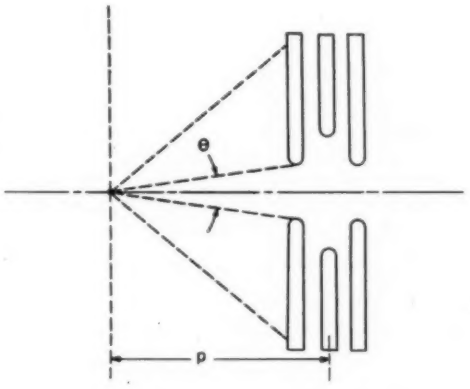

FIG. 6. Point source in front of lens.

These two extreme pictures: (1) The specimen acts as a source of electrons which completely and

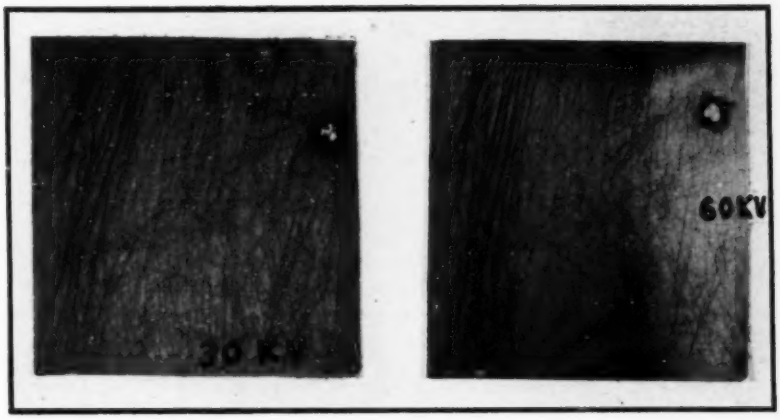

FIG. 7. Vanadium pentoxide at two different accelerating voltages.

uniformly fills the opening angle of the lens; (2) the specimen allows the electrons to pass through undisturbed in angle from their initial paths after leaving the gun—may be used also to see how depth of focus referred to the object plane is dependent upon the choice of the number of stages of magnification. For a specified resolution, it can easily be shown from elementary optics that the depth of focus in the object plane decreases as the object position approaches the lens; this, assuming that the opening angle of the objective is completely filled by the rays which are assumed to come from a point on the axis. If, on the other hand, the electrons are assumed to pass through the specimen parallel to the axis, and to retain approximately their initial angle after passing through the specimen, then obviously the depth of focus is very long no matter what number of stages is selected. Furthermore, we have already granted the possible reduction of stop diameter as the number of stages is increased to maintain a given resolution. The depth of focus will be further increased by any such stop decrease. The depth of focus will thus always increase with an increase in the number of stages for a given over-all magnification, regardless of which of these assumptions is made.

Various shielding problems may be said in general to be reduced when the number of stages is increased—largely because of the tremendous gain in simplicity of shielding that the shortened electronic chamber makes possible. Quite apart from this practical consideration of shield design is the fact that a short path allows less possibility for the cumulative action of stray fields along the entire electron path to become excessive.

METHOD OF PHOTOGRAPHY

There are two well-known methods for producing a photographic record of an electronic image. Either the film is placed in the vacuum or else a picture is produced on a fluorescent screen and a photograph of the screen is then taken from outside of the vacuum with an ordinary camera. Both methods have been used for many years in the cathode-ray oscillograph[4] art, and both methods were described in an early electron microscope patent.[5] It is quite evident that there are many advantages to be gained from the use of external photography of the image. For example, the necessity for a pre-exhausting chamber to enable photographic film to be brought into the high vacuum without unduly long delays in re-evacuating the entire chamber is entirely eliminated.

There are other considerations in the choice between external and internal photography which require considerable experimentation to evaluate. There is, for example, the question of exposure time. If the image is to be magnified electronically to the desired degree for observation and the fluorescent screen then photographed at unity magnification, the numerical aperture of available cameras is then such that the exposure time will be very long. The time duration in itself is probably not a serious objection, since the operator will lose no more time in waiting for the exposures than would ordinarily be required for insertion of photographic film. Vibration problems and stray light may, however, easily become troublesome. Of greater importance (unless one risks destroying the specimen) is that

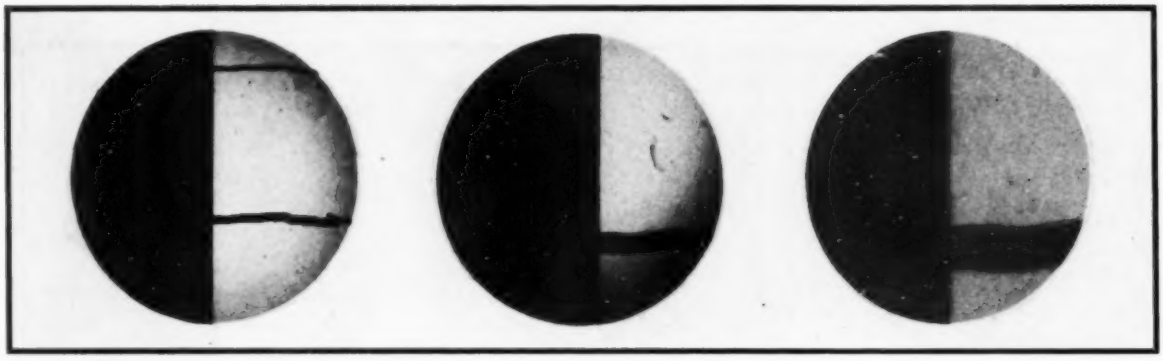

10× 25× 50×

FIG. 8. Photographs of an electron image on a fluorescent screen at various magnifications.

it is exceedingly difficult to obtain at high electronic magnification a sufficiently intense image on the fluorescent screen to make possible easy visual observation in a well-lighted room—let alone short exposure time photographs of near unity magnification.

Since the numerical aperture of a practical microscope camera increases with its magnification and, since it is highly desirable to improve radically the ease of visual observation, it is especially attractive to consider a system in which some of the magnification takes place in ordinary glass optics. Thus, as an example, for an over-all magnification of the order of 10,000×, the fluorescent screen picture might possess about 1000× magnification and the light microscope or camera might magnify another tenfold. By use of this technique, it is possible to look at the images on the fluorescent screen directly; then to view it under various magnifications easily adjusted at will from outside the instrument in the conventional light microscope manner; and finally to photograph the same fluorescent screen image which has been studied visually.

For visual observation, this scheme has an additional advantage in that glass optics have been developed to the point where very considerably greater light efficiency can be had than in the system in which the completely magnified electronic image is viewed on the fluorescent screen at about a foot's distance, as is required in the more conventional electron microscope. The improved over-all brightness in the image makes possible easy observation even at low voltages where for a goodly portion of specimens which it is desired to study in such a microscope exceedingly good contrast may be obtained. Figure 7 shows pictures of vanadium pentoxide recorded by the direct action of the beam on photographic film at two different voltages. These pictures were taken with a conventional electron microscope[6] at 4000 times magnification. As will easily be seen by noting the photographs, the lower voltage picture compares quite favorably in contrast and resolution.

All of these advantages encourage development of a fluorescent screen which will be capable of producing an image whose resolving power will stand the required light-optical magnification. Such screens have been prepared by the authors and tested for resolving power and ease of visual observation with a light microscope. It is fairly easy to obtain a fluorescent screen whose grain size will not show under 200× magnification. However, the chief problem is that electrons, even if they converge at a true point on the surface of the fluorescent screen, will not result in a point source of light. The disperson of the electrons and the resulting light sources throughout the thickness of the screen material limits the practical magnification of an image on a fluorescent screen earlier than does the grain size. Photographs of electronic images of sharp edges on the fluorescent screen are shown in Fig. 8. These indicate the feasibility of this method for a practical electron microscope design. (It should be noted, of course, that similar dispersion of light and electrons occurs in varying degrees whether the beam falls on photographic emulsion or is viewed either directly or by transmission through a fluorescent. screen.)

BIBLIOGRAPHY

(1) Part I of this paper appeared in J. App. Phys. **14**, 8 (1943).
(2) M. v. Ardenne, *Elektronen-Übermikroskopie* (Julius Springer, Berlin, 1939).
(3) J. A. Stratton, *Electromagnetic Theory* (McGraw-Hill Book Co., Inc., 1941), page 205.
(4) H. P. Kuehni and Simon Ramo, Trans. A.I.E.E. **56**, 721 (1937).
(5) R. Rudenberg, U.S. Patent No. 2,058,914, October 27, 1936.
(6) V. K. Zworykin, J. Hillier, and A. W. Vance, Trans. A.I.E.E. **60**, 157 (1941).

New Books

A Laboratory Manual of Electricity and Magnetism

By Leonard B. Loeb. Revised edition. Pp. 121+xii, Figs. 34, 15×22½ cm. Stanford University Press, Stanford, 1941. Price $1.90 (paper covered).

This laboratory manual was written to accompany *Fundamentals of Electricity and Magnetism*, by Leonard B. Loeb, the text for the third quarter of a two-year course in general physics for engineers at the University of California. It contains twelve experiments. The aims of the book are stated in the preface as follows:

1. Every experiment should have a clearly defined objective.

2. This objective should be closely coordinated with the textbook used, and should be designed to emphasize *only the most basic principles and phenomena* dealt with in the text.

3. The experiments shall at all costs be quantitative.

4. They should give the student the standard methods and techniques of making the common electrical measurements.

5. In addition to the experimental procedure, the student should be told the principles involved, the methods of achieving absolute evaluation in the c.g.s. system, precision methods available, and the reason for choosing the method of the text.

6. In order to overcome the difficulties of students who have not had the principles of the experiment in the lectures, when four experiments are run simultaneously, a complete theoretical development is given with each experiment. This does not refer to any other material and assumes that the student knows only the prerequisites of the course. If the student does not read this material before coming to the laboratory, he cannot finish the experiment in the allotted time and must postpone the experiment. This forces the student to come with some understanding of the experiment.

7. The procedure is illustrated both with schematic diagrams and perspective drawings of the apparatus and connections to make clear to the student the actual situation that confronts him on the laboratory table.

8. A form is given for the student to tabulate his results. There are five complete sets of these forms, four of which have perforations for tearing them out. A tabular report is justified on the ground that "by devising a form adequate for recording in a logical and orderly fashion the results of the measurements one not only guides the effective and orderly performance of the experiment, but also trains the student in processes of logical thinking, recording and computation." This avoids "needless copying of the text or manual or of some ancient experiment dog-eared in fraternity files." "Furthermore, the grading of problems becomes simpler, thereby reducing the assistant's load and permitting a much more uniform system of grading on the basis of accuracy tolerance."

The aims thus set forth seem to have been admirably achieved in the text. With most of the aims, one can heartily agree. The experiments are well chosen and coordinated. The results of one experiment are used in other experiments and the limitations of the method are clearly stated. Other interesting experiments not done in the text, which the student might wish to do later, are suggested.

In the complete theoretical treatment, as is to be expected, the derivation of the more complicated formulas is referred to the text. This was not supposed to be done according to aim (6). Although in a large course it is probably necessary to report the experiment by filling in a form, as in aim (8), this tends to make the experiment routine and discourages independent thinking on the part of the student. In writing up laboratory experiments, the student has his only opportunity to present material in his own words. The ability to write a good report is sadly lacking in most students. The reports do not have to be long, and they certainly should not be copied, but a statement by the student of what the experiment is all about will give him much needed practice in scientific expression. The student is often required by other instructors to write the report before leaving the laboratory.

With elementary apparatus, grades on the basis of an accuracy tolerance are somewhat a matter of chance. Tolerances could be set up suitable to the apparatus, and the student held to these limits with grading on an all or none basis. One is not going to reproduce the results of the Bureau of Standards in the elementary laboratory. What the student should learn is the principles, why the results are not more accurate, and what to do if he wants to make them more accurate. He should be expected to get results only within the limits of his apparatus by exercising proper care and technique. The statements and derivations in some cases might be made clearer to the students. For example, in the middle of page 36, it is not clear how one obtains the resistance by letting an e.m.f. flow in a coil. These and other minor errors in the text can be rectified as they are brought out by the students.

The author apologizes for the drawings. This seems unnecessary as the connections are clear and should enable

the student to set up the experiments correctly. There is a phrase in Exp. 10, "through simple reasoning for which there is no place in this experiment," which will be sympathetically interpreted by the students, perhaps not quite as it was intended.

Limitations on the choice of experiments were set by the apparatus available at the University of California in 1935. There are two improvements which probably the author would make: a current balance would be used for the absolute measurement of current instead of the tangent galvanometer in Exp. 3; and a calibrated variable inductance in Exp. 12 would make it possible to use a bridge circuit which the student could understand, rather than the Anderson bridge for which the theory is "unfortunately beyond the scope of this course." There are no experiments on electronics.

This manual is well done. It should be helpful to all those interested in fundamental electrical measurements.

C. W. UFFORD
Allegheny College

Here and There

Awards and Honors

The Edison Medal for 1942 has been awarded by the American Institute of Electrical Engineers to Dr. Edwin Howard Armstrong, Professor of Electrical Engineering at Columbia University, for distinguished contributions to the art of electric communication, notably the regenerative circuit, the superheterodyne, and frequency modulation.

The Institute of Aeronautical Sciences has selected Igor I. Sikorsky, noted aircraft designer and engineering manager of the Voight-Sikorsky Aircraft Division of United Aircraft Corporation, Stratford, Connecticut, as recipient of the Sylvanus Albert Reed Award for 1942 in recognition of his "creation and reduction to successful practice of a helicopter of superior controllability."

Edwin C. Wells, principal contributor to the design and engineering work on the flying fortresses manufactured by the Boeing Aircraft Company of Seattle, will receive the Lawrence Sperry Award of the Institute of Aeronautical Sciences. The citation reads: "For outstanding contributions to the art of airplane design with special reference to four-engined aircraft."

Orville Wright was elected an honorary member of the British Institution of Mechanical Engineers in recognition of his "distinguished contribution to mechanical science."

The *London Times* reports that the King of England has approved the recommendations of the Council of the Royal Society awarding royal medals for 1942. Those awarded among the physical sciences include: the Rumford Medal to Dr. G. M. B. Dobson, F.R.S., for his work on the physics of the upper air; the Davy Medal to Professor C. N. Hinshelwood, F.R.S., for his work on the mechanism of chemical reactions; and the Hughes Medal to Professor Enrico Fermi for his contributions to the field of electrical structure of matter, his work on quantum theory, and his studies of the neutron.

★

Recent Staff Changes

Dr. D. P. Morgan has been appointed Director of the Chemical Divisions of the War Production Board. He was formerly chemical consultant for Scudder, Stevens, and Clark of New York.

Dr. Jack Sherman, who has leave of absence from the research laboratories of the Texas Company, is now working as physical chemist for the National Defense Research Council, Office of Scientific Research and Development.

Dr. F. H. Garner, for many years chief chemist of the Anglo-American Oil Company, has been appointed to the chair of oil engineering and refining at the University of Birmingham, England. This chair was made vacant by the death of Professor A. W. Nash.

Dr. Lewis Selkirk Coonley, Associate Professor of Chemical Engineering at the Rensselaer Polytechnic Institute, has been made chairman of the department. His predecessor was Dr. Albert Watson Davison, who is now Director of Research for the Owens-Corning Fibreglas Corporation.

Dr. Thomas T. Read, formerly Vinton Professor of Mining Engineering at Columbia University, has been appointed consultant in the education and allocation of engineering in the War Manpower Commission.

★

Society News

At the 1942 annual meeting of the British Rheologists' Club, the following officers were elected: President, Dr. C. F. Goodeve; Honorary Secretary, Dr. G. W. Scott Blair; Honorary Treasurer, Dr. V. G. W. Harrison.

At the 280th anniversary meeting of the Royal Society, Sir Henry Dale was re-elected president.

Per K. Frolich, President-Elect of the American Chemical Society during 1942, succeeded Harry N. Holmes as President on January 1, 1943. Newly elected officers of the Society for 1943 are the following: President-Elect, Thomas Midgley, Jr.; Director, fourth district, L. H. Adams; Director, sixth district, R. E. Swain; Director-at-Large, Walter A. Schmidt; Councilors-at-Large, M. L. Crossley, Vincent du Vigneaud. W. Albert Noyes, Jr., and R. L. Shriner.

Dr. Hugh L. Dryden, Editor of the *Journal of the Institute of Aeronautical Sciences*, has been elected president of the Institute. He has been associated with the National Bureau of Standards for twenty-four years.

National Conference of Electron Microscopy

R. Bowling Barnes, of the Stamford Research Laboratories of American Cyanamid Company, was elected first president of the National Conference of Electron Microscopy, which was founded by leading workers in this field at the recent National Chemical Exposition held in Chicago, November 27 and 28. Other elected officers are the following: Vice President, Albert F. Prebus, Ohio State University; Secretary-Treasurer, Charles Banca, RCA Manufacturing Company; Directors, V. K. Zworykin, RCA Manufacturing Company and O. S. Duffendack, University of Michigan.

G. L. Clark, University of Illinois, presided at the formation meeting. Among the topics discussed then was the use of the electron supermicroscope for electron diffraction and for the examination of bacteria, cells, rubber, synthetic rubber, cellulose, colloids, powders, clays, ores, smokes, oils, etc.

★

Fellowship Open

The second Sigma Delta Epsilon Fellowship of $1000 has been authorized for the year 1943–1944. Women with the equivalent of a Master's degree, conducting research in the physical, mathematical, or biological sciences, who need financial assistance to complete their work for the doctorate, are eligible. Application blanks may be obtained from Dr. Eloise Gerry, c/o U. S. Forest Products Laboratory, Madison, Wisconsin, and must be submitted with references in triplicate before March 1, 1943.

★

New Courses Offered

Several new courses on ultra-high frequency and cathode-ray circuits are announced by the Graduate Electrical Engineering Department of the Polytechnic Institute of Brooklyn, as part of the War Training Program of the U. S. Office of Education. Courses are now being offered on Theory of Cathode-Ray Circuits, Experiments in Cathode-Ray Circuits, Introduction to Microwave Theory, Introductory Experiments in Microwaves, and Theory of Ultra-High Frequency Generators and Receivers. Registration is still open for courses in Experiments in Ultra-High Frequency Generators and Receivers, and Measurements at Ultra-High Frequencies. Application for admission should be made on blanks obtainable from the Graduate Electrical Engineering Department, Polytechnic Institute of Brooklyn, 85 Livingston Street, Brooklyn, New York.

★

Engineering College Research Association

An Engineering College Research Association has been formed by seventy-three engineering colleges to aid the government and industry in the war effort. It will attempt to use the facilities of these schools for war research and post-war experimentation and is designed to eliminate duplication by bringing together industrial and academic research. Dean W. R. Woolrich of the College of Engineering of the University of Texas is the chairman. The first meeting was held in Washington, November 27.

★

New Standard Letter Symbols for Mechanical Terms

The American Standards Association has published an approved American Standard for letter symbols for mechanics of solid bodies. There are sixty-eight letter symbols to indicate such terms as angular acceleration, circular frequency, factor of safety, normal strain, wave-length, and in addition the new standard cites general principles of letter symbol standardization governing manuscripts, subscripts, superscripts, unlisted magnitudes, and typography. The work was done by a committee composed of representatives from the American Association for Advancement of Sciences, the American Institute of Electrical Engineers, the American Society of Civil Engineers, the American Society of Mechanical Engineers, and the Society for the Promotion of Engineering Education.

★

New General Office

Fish-Schurman Corporation, manufacturers of raw optical, technical, and scientific glass, and scientific instruments, announce the moving of their General Offices to 230 East 45 Street, New York City.

★

Necrology

Professor Alfred Baker, Professor emeritus of Mathematics at the University of Toronto and past president of the Royal Society of Canada, died on October 27 at the age of ninety-four.

Dr. William Martin Blanchard, Professor of Chemistry and Dean emeritus of the De Pauw University College of Liberal Arts, died on December 21 at the age of sixty-eight.

Dr. Hans G. Beutler, research associate in physics at the University of Chicago, died on December 15 at the age of forty-six. Dr. Beutler, a well-known spectroscopist, came to this country in 1936 from the Kaiser Wilhelm Institute for Physical Chemistry in Berlin.

Professor Carl Dorno, founder and director of the Physical Meteorological Observatory at Davos, Switzerland, died recently at the age of seventy-seven.

Charles W. Frederick, head of the science division of the lens factory of Eastman Kodak Company of Rochester, New York, died on November 29, at the age of seventy-two.

Dr. Harrison E. Howe, Editor of *Industrial and Engineering Chemistry* for twenty-one years, died on December 10 at the age of sixty.

Professor Wilmot V. Metcalf, who taught physics and chemistry and specialized in the field of physical chemistry, died November 21 at the age of eighty-two.

Contributed Original Research

The Ploughing and Adhesion of Sliding Metals

F. P. Bowden, A. J. W. Moore, and D. Tabor
Council for Scientific and Industrial Research, East Melbourne, Australia
(Received November 21, 1942)

Studies of the surface damage caused by the sliding of clean metals on one another show that penetration and distortion occur to some depth beneath the surface. Micro-examination shows that welding of the metals takes place quite readily even at low speeds of sliding when the surface temperature-rise due to frictional heat cannot be very high. In some cases the welded junctions may pluck out portions of the harder metal. These and other results have led to a more quantitative theory of metallic friction. It is suggested that in general the frictional force between clean metal surfaces is made up of two parts. The first is the force required to shear the metallic junctions formed between the surfaces; the second is the ploughing force required to displace the softer metal from the path of the harder. By using steel sliders of various shapes and sizes on a soft metal like indium, these two factors have been estimated separately, and it is shown that an approximate calculation of the friction between metal surfaces may be made in terms of the known physical properties of the metals. The effect of surface contamination is also discussed.

THE SURFACE DAMAGE CAUSED BY SLIDING

WHEN metal surfaces slide on one another, penetration and distortion of the metals occur to some depth beneath the surface. The frictional force and the nature of sliding are both influenced by the bulk properties of the metals, and the friction cannot be regarded as a purely surface effect. It has been suggested[1] that the frictional resistance between unlubricated metals is due, primarily, to the shearing of the metallic junctions formed by adhesion and welding at these points of contact, and to the work of dragging or ploughing the surface irregularities of the harder metal through the softer one. Although the metals may be very carefully polished, hills and valleys which are large compared with the dimensions of a molecule will still be present on the surface. Contact will occur only locally at the summits of these irregularities. The high pressures at these points of contact will readily cause local adhesion and welding between the metals.

The nature and extent of this welding and ploughing may be determined if a careful micro-examination of the surface is made after sliding has occurred. The usual method of micro-examination of a metal surface by cutting a section at right angles to it or by examining the surface direct will not reveal very fine surface irregularities. Nelson[2] has described a technique which may be used to give more detailed information about the surface contours. In this method the metal surface is first protected by depositing on to it a layer of another metal of similar hardness and a section is then cut at a very oblique angle to it. If the section is cut at an angle of about six degrees to the surface it gives a contour of the surface with its vertical component magnified about ten times. Figure 1 shows the contour of a section across the track formed on a flat mild steel surface (hardness 120 B.H.N.), after a slightly worn spherical slider of the same metal has passed over it once.

The section was cut at right angles to the direction of sliding. The load was 4000 g, the initial radius of curvature of the slider was 0.3 cm and the surface speed was very slow, about 0.01 cm/sec. The steel was unlubricated and the coefficient of friction was *ca.* $\mu=0.7$. The width

[1] Bowden and Leben, Proc. Roy. Soc. **A169**, 371 (1939); Phil. Trans. Roy. Soc. **A239**, 1 (1940); Bowden and Tabor, "Council for scientific and industrial research" (Australia), Bulletin No. 145 (1942).

[2] Nelson, "Conference on friction and surface finish." Mass. Inst. Tech. p. 217 (1940).

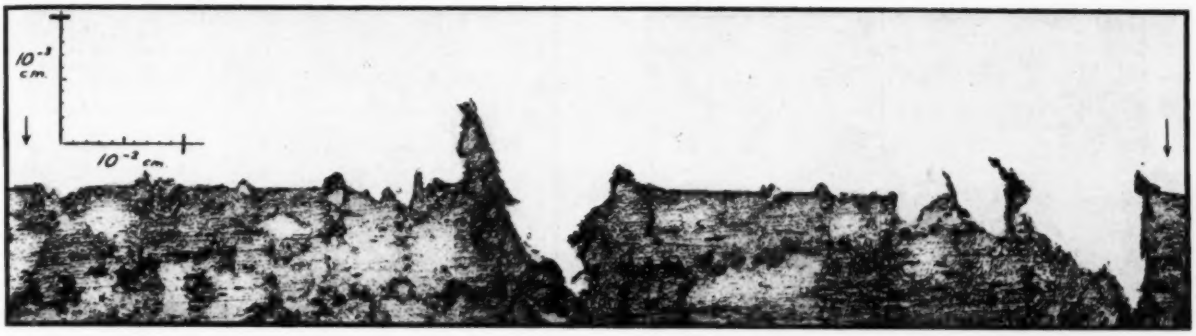

FIG. 1. Taper-section of track formed by sliding a hemispherical steel rider on an unlubricated steel surface. Original photograph has a horizontal magnification of 200 and a vertical magnification of 2000. The width of the track is indicated by the arrows. The tearing and plucking of the steel are clearly seen.

of the track is indicated by arrows. The horizontal magnification on the original photograph (reproduction is approximately $\frac{3}{4}$ size) is 200 and the vertical magnification 2000.

The localized nature of the damage is at once apparent. A considerable area of the surface is unchanged. At a number of points, however, penetration, ploughing and tearing of the metal have occurred. The depth of these torn channels varies from considerably less than 10^{-4} cm to about 10^{-3} cm. At other points on the surface the metal is raised above its former level. Some of this torn metal comes from the lower surface and some of it is probably left behind by the slider.

If the upper surface is of a softer metal, this ploughing out is not observed. Instead small fragments of the softer metal are left welded on the harder one. Characteristic welded junctions of this type, formed when copper (hardness 60 B.H.N.) is slid on mild steel at a low speed are shown in Fig. 2. The section was again cut at right angles to the direction of sliding, and the conditions were similar to those used on the steel surface. The coefficient of friction in this case was about 0.8. The horizontal magnification is 200, and the vertical magnification 2000. The greater part of the steel surface was undamaged, and isolated fragments of copper were left adhering to the steel and distributed over it. For these junctions the shearing has occurred in the copper itself. In other cases, for example the hollows and pits *H*, shown in Fig. 2, the copper has *plucked*

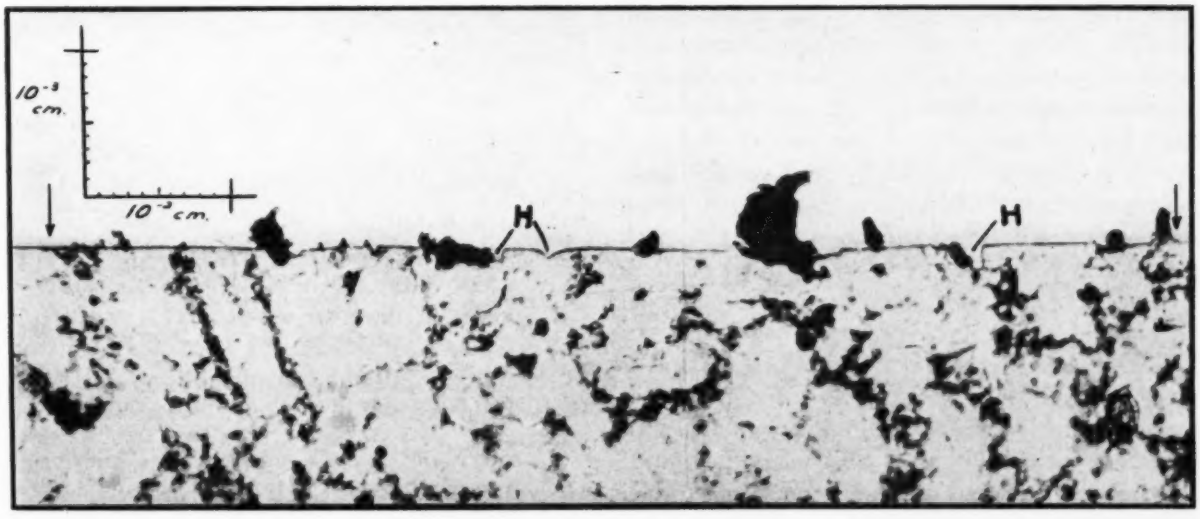

FIG. 2. Taper-section of track formed by sliding a hemispherical copper rider on an unlubricated steel surface. Horizontal magnification 200. Vertical magnification 2000. The width of the track is indicated by arrows. Note the adhering fragments of copper, and the pits marked *H* where the steel has been plucked out of the surface.

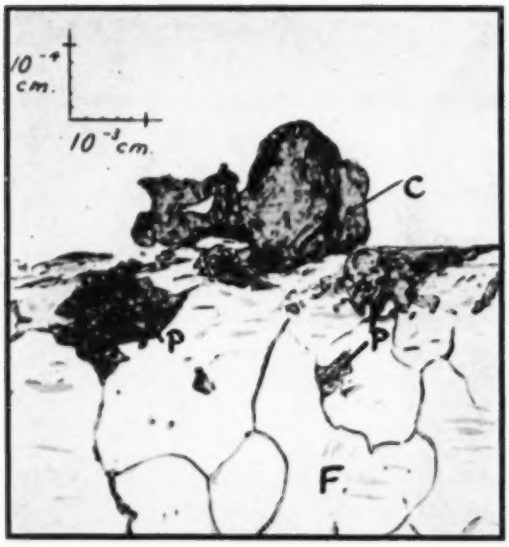

FIG. 3a. Taper-section of portion of track formed by copper on steel. The copper fragment shown has welded firmly on to the steel surface and shearing has taken place within the copper itself. Horizontal magnification 1000. Vertical magnification 10,000. F = Ferrite, P = Pearlite, C = Copper.

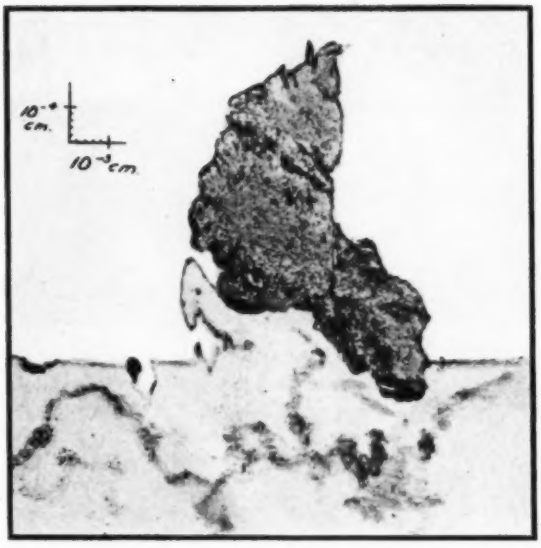

FIG. 3b. Taper-section of another portion of track formed by copper on steel. This shows again the welding of the copper on to the steel, and the way in which the steel has been distorted and plucked out by the copper. Horizontal magnification 500. Vertical magnification 5000.

out small fragments of the steel. Microphotographs of the copper steel junctions at higher magnifications are shown in Figs. 3a and 3b. The white portion of the steel in Fig. 3a is ferrite, the dark portion P is pearlite, and C is a copper fragment *ca.* 10^{-3} cm wide and *ca.* 10^{-4} cm high. It is clear that the copper is welded on to the steel and that the junction has sheared in the copper itself. A similar copper fragment is shown in Fig. 3b. It is seen that the forces which sheared through the copper have also caused appreciable deformation of the underlying steel, and have actually raised portions of the steel above the general level of the steel surface. Over a large portion of the surface, however, the break has occurred between the copper and the steel, so that there is no apparent change in the surface.

The wear of a hard metal by a soft one which is brought about in this way by a welding and plucking action is a much slower process and is very different in appearance from the more normal abrasive wear produced by rubbing with a harder surface. Figure 4 at a magnification of 100 shows the wear produced on a hard steel surface (hardness 600 B.H.N.) after sliding for a distance of 1000 cm of copper. The plucking is clearly seen.

THE SURFACE TEMPERATURE OF SLIDING METALS

In these experiments the sliding speed was low, so that the surface temperature was sensibly the same as that of the bulk metal. When the sliding speeds and loads are sufficiently great the frictional heat may raise the local surface temperature to a high value so that a softening or even melting of the metals may occur at the points of intimate contact. This will assist the welding process. The occurrence of these high temperatures has been demonstrated by measurements of the thermal e.m.f. developed between dissimilar metals sliding on one another[3] and by polishing experiments.[4] They have also been confirmed recently by other workers.[5–7] These observations are of importance since they mean that, under many of the conditions of load and speed used in practice where the temperature rise is undoubtedly high, the frictional behavior of the metals, and of lubricant films on them will be determined not by their properties at room

[3] Bowden and Ridler, Proc. Roy. Soc. **A154**, 640 (1936).
[4] Bowden and Hughes, Proc. Roy. Soc. **A160**, 575 (1937).
[5] Thomson and Logan, J. Roy. Tech. Coll. Glasgow **4**, 696 (1940).
[6] Matthew, J. Roy. Tech. Coll. Glasgow **4**, 360 (1940).
[7] Beeck, Givens, and Williams, Proc. Roy. Soc. **A177**, 103 (1941).

temperature, but by their properties at the actual temperature of sliding. If the loads are light, however, or the sliding speed slow, the temperature rise will be of the order of only a few degrees. This was pointed out in the original paper[3] where the conditions necessary for high temperatures were given, but it needs emphasizing here since some misunderstandings seem to have arisen on this point. Other workers[8,9] have shown that when the average speed of sliding is slow, the momentary temperature rise is of the order of 30–50°C. This is in agreement with our observations and it is clear that a temperature rise of this order will be insufficient to affect sensibly the mechanical properties of the metals. Nevertheless, for these low speeds, and even for stationary surfaces, adhesion and welding of the metals at the local points of intimate contact will occur.

INTERMITTENT SLIDING

In much of this work the friction was measured on an apparatus which consisted essentially of a lower flat surface and an upper curved surface resting on it. A photograph of such an instrument is shown in Fig. 5. The lower surface is driven along at a uniform rate by a water piston. The upper surface is supported by a spring device for applying the load, and a bi-filar suspension for measuring the frictional force. The inertia of this system is small, so that it is capable of responding readily to any rapid fluctuations in the frictional force which may occur between the sliding surfaces. It was found that with such an instrument, in which one part possesses an appreciable degree of elastic freedom, the motion may not be continuous but may be intermittent and proceed by a process of "stick-slip." This necessarily means that the kinetic friction during the "slip" is less than the static friction at the "stick." The nature of the motion will, of course, depend on the mechanical properties of the moving system. Other workers,[8,9] repeating some of these experiments with similar apparatus, find results which are similar but they lay particular stress on the fact that the motion is determined by the elastic properties of the system. This had, however, already been emphasized by the writers, e.g., reference 10, where it is stated that the motion "will be influenced by the mechanical properties of the system such as the natural frequency, the moment of inertia, and the damping of the moving parts. Finally, it will be influenced by the velocity of the main forward motion." Undoubtedly, however, with any particular mechanical system the type of sliding is profoundly influenced by the nature of the metals and of the lubricant films on the surface. Even when the top surface is held on a massive steel bar, some degree of intermittent motion may be observed.[10] Since many moving systems possess an appreciable degree of elastic freedom and since, in the limit, the surface irregularities, themselves, may be capable of a small elastic deformation, this "stick-slip" motion is of frequent occurrence provided the surfaces and other conditions are suitable. It is not suggested that the occurrence of "stick-slip" is in itself proof that a lubricant is a poor one, although most

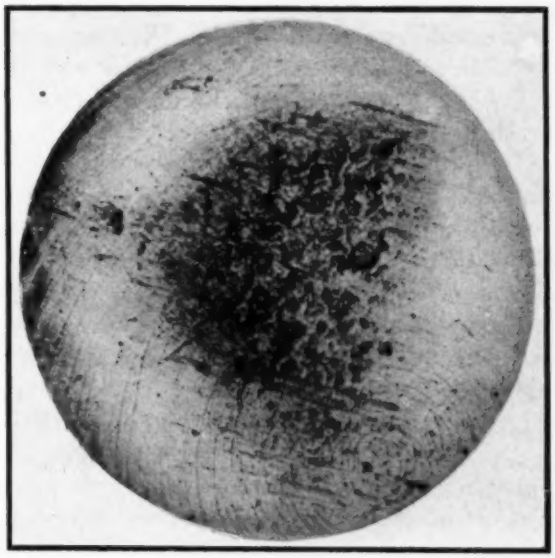

FIG. 4. Worn portion of a hemispherical steel slider after it has traversed 1000 cm of track on a copper surface. The plucking away of the steel is clearly seen. Magnification 100.

[8] Morgan, Muskat, and Reed, J. App. Phys. **12**, 743 (1941).

[9] Bristow, Nature **149**, 169 (1942). See also Blok, J. Soc. Aut. Eng. **46**, 54 (1940), on the theory of relaxation oscillations, and the experimental work of Papenhuyzen, de Ingenieur **53**, 75 (1938), and earlier work by Kaidanovsky and Haykin, Zeits. f. Physik **3**, 91 (1933).

[10] Bowden, Leben, and Tabor, Engineer **168**, 214 (London, 1939).

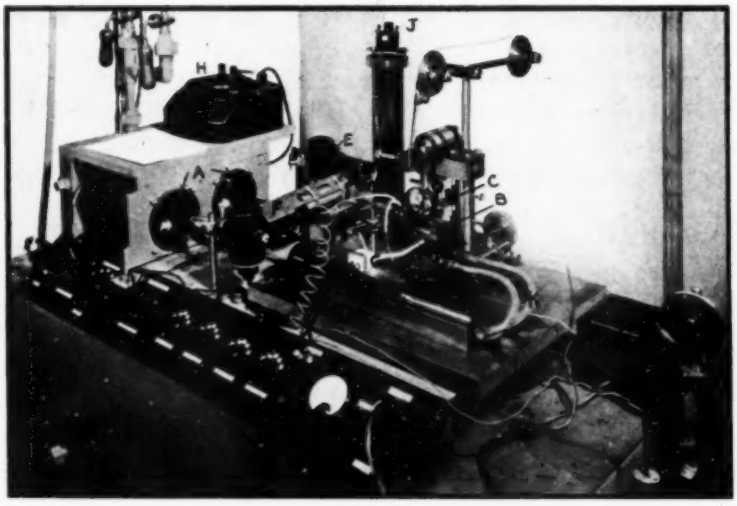

FIG. 5. Apparatus for measuring and analyzing the friction between slowly moving surfaces, with and without lubricants, at room temperature and at elevated temperatures. A = Water-driven pistons for driving the lower surface at a slow steady speed. B = Lower surface (flat). C = Upper curved surface held in spring-loading device and attached to a bifilar suspension. D = Surface thermocouple. E = Light source for recording friction. F = Light source for recording surface speed. G = Leads to heating element for heating lower surface. H = Galvanometer for giving visual readings of surface temperature. J = Galvanometer for recording surface temperature simultaneously with friction. K = Rubber tubing to cooling system below heating element. The recording camera is not shown in this figure.

poor lubricants give a motion of this type if the mechanical system will permit it. The nature of the sliding, the value of the friction and the damage to the surface and other factors must all be taken into account.

AMONTONS' LAW

Another problem that is of general interest is the relation between the frictional force, the area of contact, and the load. The early work of Coulomb and of Amontons led to the formulation of two "laws," (i) that the frictional force was independent of the area of the sliding bodies, and (ii) that the frictional force was proportional to the applied load.[11] There has been some difficulty in explaining these laws, but experiments on the real area of contact between stationary and between moving surfaces offer a theoretical explanation of them. In these experiments[12] the area of contact between the metals was determined by measuring the electrical conductance between them, and the results showed that, in general, contact occurred only locally at the summit of the surface irregularities so that the real area of contact was very small and was almost independent of the apparent area of contact. We should, therefore expect that the frictional force would also be independent of the apparent area of contact.

The second law, which is often referred to as Amontons' law, also presented difficulties, since it was usually assumed that when the load was applied the surface was deformed elastically. In this case, the area of contact and hence the frictional force would be expected to vary as the two-thirds power of the load and not as the first power.[13] The conductivity measurements, however, showed that the deformation of the surfaces was mainly *plastic*.[12] The metals flowed under the applied load until the area of contact was sufficient to support it. In the case of plastic flow the area of contact is directly proportional to the applied load, so that the difficulty disappears and we should expect the second law (Amontons' law) to hold.

In the earlier experiments a variation in the load automatically produced a change in the area of contact. It was not possible to vary them independently. An artificial method of doing this has been used and the experiments described below show that under these conditions Amontons' law breaks down completely. If the area of contact is kept constant, the frictional force is also constant and is independent of the applied load. It is clear that the frictional resistance is determined, primarily, by the real area of contact and that the load is important only insofar as it affects this area.

[11] Hardy, *Collected Works* (Cambridge University Press, London, 1936).
[12] Bowden and Tabor, Proc. Roy. Soc. **A169**, 391 (1939). Also see Tabor, "Dissertation" (Cambridge, 1939).
[13] Adam, *Physics and Chemistry of Surfaces* (Oxford University Press, London, 1938), p. 232.

CALCULATION OF FRICTION

Although the physical processes that occur during sliding are obviously very complex, these and other experiments have led to the development of a theory of metallic friction on a more quantitative basis which enables us, in certain cases, to make an approximate calculation of the friction between clean metal surfaces in terms of the known physical properties of the metals. It has been suggested that we may, in general, write the frictional force F as $F=S+P$, where S is the force required to shear the metallic junctions and P the force required to displace the softer metal from the path of the slider. It follows that $S=As$ where A is the real area of contact of the metals and s the shear strength of the softer metal, while $P=A'p$ where A' is the cross section of the torn track and p is the "flow pressure," i.e., the pressure to cause plastic flow of the softer metal. From this $F=As+A'p$.

When the load is applied to the surfaces, plastic flow of the softer metal occurs at the regions of contact until the area of contact is sufficiently great to support the applied load. With any particular metal, therefore, the real area of contact is determined, primarily, by the load W, and $W=pA$.

Hence $F=Ws/p+A'p$ and the coefficient of friction is

$$\mu=\frac{F}{W}=\frac{s}{p}+\frac{A'p}{W}=\frac{\text{shear strength}}{\text{flow pressure}}+\frac{A'p}{W}.$$

If the ploughing term is negligible, it follows that

$$\mu=\frac{\text{shear strength}}{\text{flow pressure}}.$$

A somewhat similar expression applied to the cutting of metals has recently been developed by Ernst and Merchant.[14]

An experimental investigation of these relations has been made for steel sliding on indium which is a soft metal. By using steel sliders of various shapes and sizes, it has been possible to calculate F, S and P in terms of the flow pressure and shear strength of the softer metal.

[14] Ernst and Merchant, "Conference on friction and surface finish," Mass. Inst. Tech. p. 76 (1940).

If we consider, for example, a steel sphere resting on a plane surface of indium, it will sink into the softer metal until the area of contact between the surface is sufficient to support the applied load and in that case

$$W=pA, \tag{1}$$

where A is the projected area of contact. The force F required to move the slider forward in a direction parallel to the surface will be made up of two factors. The first is the force P required to displace the softer metal from the front of the slider, and will be equal to the cross-sectional area of the grooved track multiplied by the flow pressure of the softer metal.

$$P=\frac{1}{12}\frac{d^3}{r}p, \tag{2}$$

where d is the track width and r is the radius of curvature of the hemisphere (see Figs. 6a and b).

The second factor is the force S required to shear the metallic junctions at the points of adhesion between the two metals. Then

$$S=As, \tag{3}$$

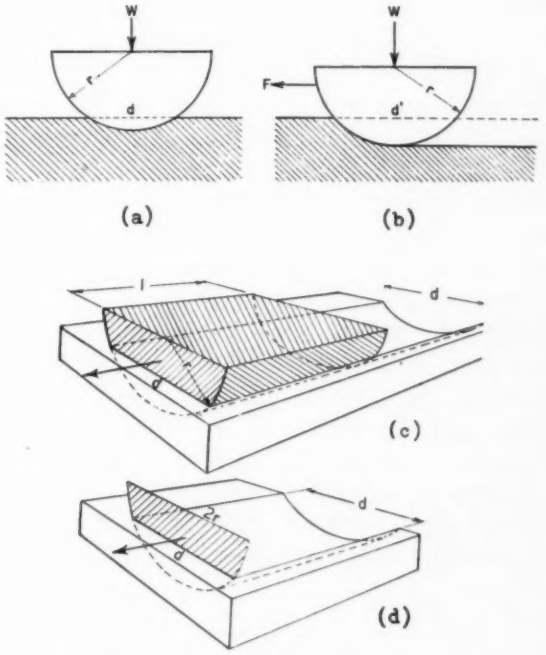

FIG. 6. Deformation of a soft metal by a hard curved surface. (a) Hemisphere, stationary. (b) Hemisphere, moving. (c) Horizontal cylinder normal to direction of motion. (d) Flat spade normal to direction of motion.

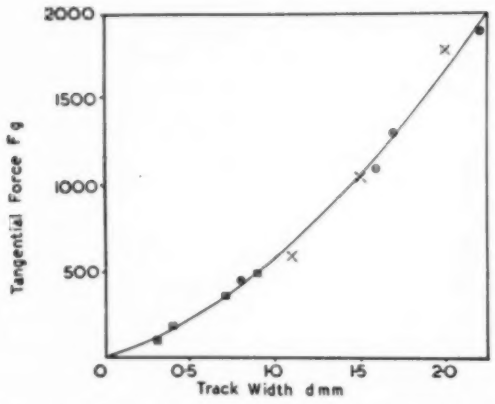

FIG. 7. Friction of steel on indium determined by three methods. × Steel sphere under load on indium surface. ⊙ Steel sphere held rigidly on indium surface. ⊡ Steel sphere under load on thin indium films deposited onto hard steel substrate.

where s is the force per unit area which, acting in a direction tangential to the interface, is required to shear the junctions. Hence

$$F=P+S=\frac{d^3}{12}\frac{p}{r}+sA. \tag{4}$$

From this we see that if the work of ploughing is small, Amontons' law will hold, since F will then be equal to sA and the coefficient of friction

$$\mu=F/W=s/p=\text{constant}. \tag{5}$$

It is clear that this general relationship should hold whatever the initial shape of the sliding surfaces. Under most normal experimental conditions, P is not very large compared with S, so that the deviations from Amontons' law are not usually very marked.

As another type of slider, we may consider a cylinder of hard metal resting on a plane surface of a soft metal (Fig. 6c). It is clear that the ploughing term P will be equal to the area of the submerged segment of the front of the cylinder multiplied by the flow pressure. The shearing term S will be equal to the area of the curved surface that is submerged, multiplied by s, so that to a first approximation

$$F=\frac{1}{12}\frac{d^3}{r}p+sdl, \tag{6}$$

where r is the radius of the cylinder and l its length.

If the length of the cylinder is zero, i.e., if the slider is in the form of a semi-circular spade (Fig. 6d), the work of shearing vanishes, and all the frictional work is due to ploughing, and

$$F=\frac{1}{12}\frac{d^3}{r}p. \tag{7}$$

By using conical sliders and plane sliders, similar relationships may be deduced.

THE INFLUENCE OF LOAD ON THE FRICTION OF A SPHERICAL SLIDER

It is assumed in the theory that the frictional resistance is determined by the real area of metallic contact and by the work of displacing the metal and that the applied load is important only insofar as it affects these quantities. It will be seen from Eq. (4) that, for a spherical slider on a plane surface, the frictional resistance in the case of two particular metals should depend only upon the track width d.

Experiments were, therefore, carried out to test this. The upper spherical surface was of steel and the lower plane one of indium. The experiments were made in three distinct ways.

(i) The friction was determined in the usual manner. The load was applied to the spherical slider and a measurement made of the force required to slide it over the indium. The tangential force was plotted against the track width d and the results are marked × in Fig. 7.

(ii) The spherical slider was held rigidly in a horizontal plane and was sunk a small but

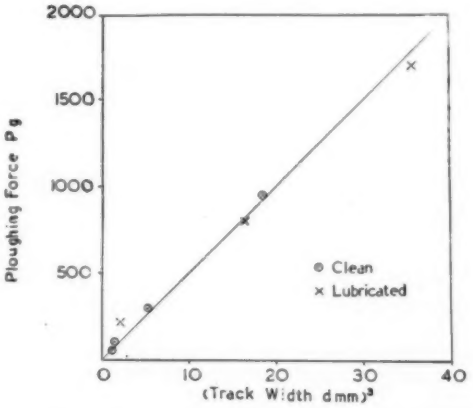

FIG. 8. Force P required to plough through indium with flat steel spade, as function of track width d. It is seen that P is proportional to d^3.

definite depth into the indium surface. The force required to slide it was then measured and the measurements were repeated at a number of definite depths. Again the tangential force was plotted against d and the results marked ⊙ are shown in Fig. 7. It will be seen that the points lie on the same curve.

(iii) The indium was electroplated onto a plane surface of hard tool steel so as to form a film of definite thickness. The spherical slider was placed on top of this, different loads were applied and the friction measured.

When the load is applied the spherical surface will sink through the indium layer until it is supported by the underlying steel surface. Since the steel surfaces are deformed comparatively little by the load, further increases in load will have relatively little influence on the area of contact between the slider and the indium and d will now be almost independent of load. Provided a very thin layer of indium still adheres to the bottom surface so that no steel-to-steel contact occurs we should expect *the frictional force to be almost independent of the applied load*. Experiment showed this to be the case. The frictional force showed comparatively little change when the load was varied by a large factor. For example, with a load of 500 g the frictional force F required to slide a steel hemisphere on an indium film 4×10^{-4} cm thick plated onto tool steel was 100 g. When the load was increased to 8000 g (i.e., by a factor of 16) the frictional force F only increased to 300 g. This means that the coefficient of friction as usually defined by $\mu=F/W$ had fallen from $\mu=0.2$ to $\mu=0.04$. The most convenient way of varying d is to vary the thickness of the indium coating. Experiments were made with thicknesses ranging from 10^{-5} to 10^{-3} cm. The tangential force was plotted against d and the results marked ⊡ are shown in Fig. 7. It will be seen that the results again lie on the same curve.

The measurements obtained by these three different experimental methods all give the same results. When F is plotted against the track width d the points all lie on the same smooth curve. It is clear that the frictional force is determined by d and not by the load or the method of measurement so that the theoretical assumption made at the beginning of the paper is justified.

THE PLOUGHING TERM P, AND THE FLOW PRESSURE p

The theory shows that the ploughing force P should, in the case of the spade, be proportional to the cube of the track width d. In Fig. 8 the measured value of the tangential force required to pull the spade along is plotted against d^3. It will be seen that the experimental results are in good agreement with the theory and the points lie on a straight line.

Since P represents the work of ploughing out the metal its value should not be influenced by

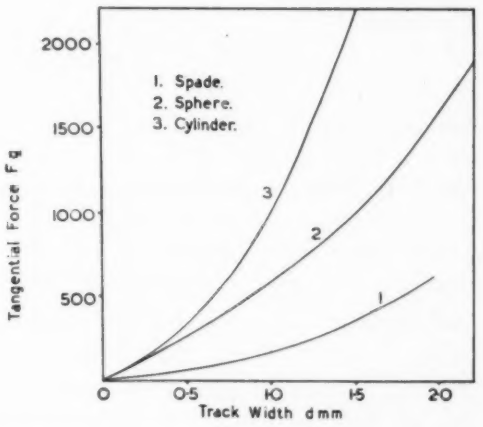

FIG. 9. Friction F of steel surfaces on indium as function of track width d. 1. Spade. 2. Sphere. 3. Cylinder.

the presence or absence of a lubricant. The experiment was, therefore, repeated with the surfaces flooded with oleic acid. The results obtained are represented on the graph by the points marked ×. It will be seen that they lie on the same straight line, and it is clear that the lubricant has little or no effect on P. Under certain conditions, when the accumulated metal piles in front of the slider, a lubricant will influence P.

By using Eq. (7), we may calculate the flow pressure of the metal and compare it with the value obtained in other ways.

From Eq. (7) we have

$$p=\frac{P}{d^3}12r,$$

where P/d^3 is given experimentally from the

slope of the curve in Fig. 8 and is equal to 50. Substituting in the above equation we obtain $p=1500$ g/mm. The value obtained from a static indentation test was 1000 g/mm² so that the agreement is reasonable. Since the ploughing experiment measures the pressure required to cause flow of the metal at an appreciable rate and the indentation test measures it under static conditions, we should expect the former value to be somewhat higher. Increasing the ploughing speed by a factor of 200 caused p to increase from 1.5 to 2.8 kg/mm², i.e., by a factor of less than 2.

As sliding proceeds the displaced metal accumulates in front of the spade and increases the area of contact so that the ploughing force increases with time. For this reason all these measurements were made in the initial stages of sliding.

From these results and the results of the next section, it is evident that the ploughing term may constitute an appreciable fraction of the total friction. For example, with a small hemispherical slider on indium it may amount to as much as one-third of the total friction. If a harder metal is used the penetration for a given load will be less, but since the flow pressure is higher, the resistance to ploughing may still be considerable. Analysis suggests that with a hemispherical slider on metals of different hardness, P should be proportional to $1/\sqrt{p}$ so that it will be less important for hard metals. With a conical slider, however, analysis shows that P should be independent of p. With flat surfaces making contact over a large number of points the ploughing will be distributed over a wide area. It is clear that over a wide range of experimental conditions, the work of ploughing must be taken into account.

The results show that the ploughing term may, in certain cases, be calculated in terms of the geometry of the moving parts and the flow pressure of the softer metal. The flow pressure is used in this paper as meaning the pressure to cause plastic flow of the metal. This is not a clearly defined property of a particular metal and depends upon the experimental conditions under which it is measured, the direction of flow, rate of application of pressure, the initial state of the metal, and the extent to which work hardening takes place during flow. All these factors, as well as the formation of a built-up area of the displaced softer metal in front of the slider, will influence the work of ploughing. Further, with some metals, the work hardening effect and the effect of speed may be considerable.

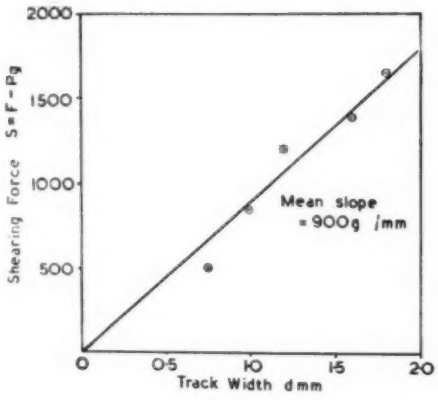

FIG. 10. Force S required to shear metallic junctions formed between steel cylinder and indium. The mean slope is 900 g/mm. Since the length of the cylinder is 4 mm, the shear strength $s=900/4=230$ g/mm².

THE SHEARING TERM S, AND THE SHEAR STRENGTH s

Force Due to Shearing

In Fig. 9 the tangential force F is plotted against the track width d for a steel sphere, a steel cylinder of length 0.4 cm, and a steel spade, all having the same radius of curvature 0.25 cm. It is seen that for a given track width the friction is least for the spade, as is to be expected, since the shearing term is clearly absent. Further, as we might expect, the friction for the sphere is intermediate in value between the spade and the cylinder.

The difference between curves 1 and 3 gives the shearing term S for the cylinder, and from Eq. (6) we see that it should be proportional to the first power of the track width d. In Fig. 10 the experimental value of S thus obtained is plotted against d. It will be seen that experiment is again in good agreement with theory, and from the slope of the curve we obtain a value of $s=230$ g/mm².

The difference between curves 1 and 2 gives,

in a similar way, the shearing term for the sphere, and this yields a value of $s = 350$ g/mm^2.

A subsidiary test was carried out to determine the force required to shear solid indium. Cylinders of indium of various diameters were sheared between two flat steel plates sliding over one another in close contact. It was found that the shearing force was proportional to the area of cross section of the cylinders, and for the same speed as that used in the above friction experiments a value of s was obtained, $s = 220$ g/mm^2. Increasing the speed of shear by a factor of 150 caused s to increase by only a factor of 2.

The results obtained from the friction measurements for a variety of experiments in which steel sliders of different shapes and sizes were used, are shown in Table I.

TABLE I. Shear strength of steel indium junctions calculated from friction. (Sliding speed = 0.005 cm/sec.)

Slider	s in g/mm^2
Small steel cylinder ($r = 0.25$ cm)	230 ± 30
Large steel cylinder ($r = 2.5$ cm)	250 ± 50
Small steel hemisphere ($r = 0.25$ cm)	300 ± 50
Large steel hemisphere ($r = 2.5$ cm)	270 ± 70
Curved indium slider on flat steel surface	325
Shear strength of pure indium	220

It will be seen that although the experimental methods were very different in each case, the values obtained for s are in reasonable agreement. *Moreover, the value of s (i.e., the shear strength of the steel indium junction) is very nearly equal to the shear strength of pure indium.*

Further a micro-examination of the steel sliders showed numerous fragments of indium that had welded on to the steel: actual shearing had occurred within the bulk of the indium itself.

These results imply that the contact between clean steel and indium is extremely intimate (see next section). In such circumstances, one might expect the shear strength as determined from friction experiments, to be higher than that obtained from shearing experiments on pure indium, for two reasons. Firstly, a considerable amount of work hardening of the softer metal occurs, particularly where the deformation is greatest, that is, in the immediate vicinity of the interface. For this reason, the thin layer of metal near the surface may be stronger, giving a higher value for s, and the shearing, when it does take place, may occur at an appreciable distance from the interface. Secondly, as Bridgman has shown, the shear strength of most metals is greatly increased when they are subjected to pressure.[15] Neither of these factors seems to be very marked for the soft pure indium used in these experiments. For harder metals, however, where the deformation and work hardening may be more marked, and where the pressures at the points of real contact may be very much higher, the increase in frictional shear strength may be considerable. This has been observed in earlier papers.[16]

THE INTIMACY OF CONTACT AND THE INFLUENCE OF SURFACE FILMS

We have seen that the frictional resistance is determined mainly by the real area of contact A between the surfaces. Under most conditions this area of contact is determined, primarily, by the load and by the flow pressure of the metals, since one or both of the solids flows until the area is sufficiently great to support the load.

Although the area of contact is, under any given conditions, determined primarily by the mechanical properties of the solids, it is clear that the *intimacy* of the contact and the strength of adhesion at the points of contact will be greatly influenced by the presence of surface films. Under most experimental conditions metal surfaces are covered with a thin oxide layer and other contaminating films, and during sliding these oxide and surface films will be torn, and some metallic contact will occur. We should expect that the adhesion and shear strength of these junctions, which consist of metal plus torn fragments of oxide and other contaminants, would be less than that of the pure metal. Earlier experiments have shown that this is indeed the case. If the oxide and surface film is removed by outgassing in a high vacuum, the friction between the metals is increased to a very high value.[17]

In the same way we should expect that the

[15] Bridgman, Phys. Rev. **68**, 824 (1935).
[16] Bowden and Leben, Proc. Roy. Soc. **A169**, 371 (1939), and especially Leben, "Dissertation" (Cambridge, 1939).
[17] Bowden and Hughes, Proc. Roy. Soc. **A172**, 263 (1939).

deliberate addition of suitable lubricant films to the metals would again diminish the intimacy of contact and the strength of adhesion at the junction. Although experiments show that this is the case, they also show that lubricant films are rarely, if ever, able to prevent some metallic adhesion from taking place. The surface irregularities penetrate and tear through the surface film, and metallic seizure and damage occur. The total area over which this metallic seizure takes place is, of course, very much smaller in the presence of lubricants than in their absence.

It is clear that, in the case of a particular junction, one or two conditions may obtain:

(1) The strength of adhesion between the soft metal and the hard may be greater than the shear strength of the soft metal. In this case the frictional force will be that required to shear the softer metal, the break will occur within this metal and fragments will be left adhering to the surface of the hard metal.

If the fraction of the total area of contact over which this occurs be α, the frictional resistance due to these junctions will then be $\alpha s_1 A$ where s_1 is the shear strength of the softer metal.

(2) The strength of adhesion at the interface between the two metals is less than that of the softer metal. In this case, slip will occur between the metals, and the soft metal will not be wiped on to the harder one. The value for the shear strength of these weaker junctions will not necessarily be constant. It may vary from a value which approaches s_1 down to very small values. Let s_2 be the average value. Then for any general case of contact between metal surfaces the total frictional force F will be given by:

$$F = A(\alpha s_1 + (1-\alpha)s_2).$$

From the fact that the shear strength of indium-steel junctions as calculated from the friction experiments is almost equal to the shear strength of pure indium, it would seem that for clean steel sliding on indium α is very nearly equal to unity, and s, to the shear strength of pure indium. On the other hand, the taper section in Fig. 2 for copper on steel suggests that the adhesion is not sufficient to cause shearing within the copper over the whole area of contact, and frequently the break occurs at the steel-copper interface. In this case α must be appreciably less than unity, and s_2 will be less than s_1.

It is probable that the main effect of adding a lubricant to clean metal surfaces is to reduce both α and s_2.

ELASTIC AND PLASTIC DEFORMATION. FRICTIONAL HYSTERESIS

The reality of the welding process is clearly demonstrated when frictional measurements are made with soft plastic metals. With lead or indium, for example, sliding on steel the value of the friction is very variable and depends on the previous history. If the load is first applied and then decreased or removed altogether, the surfaces continue to "stick" together and the tangential force necessary to cause sliding remains high, although there is no normal load applied between the surfaces. This is not observed on harder, more elastic, metals. For such metals, the frictional force decreases when the load is decreased and the effects are reversible. It has been suggested elsewhere[12] that the elastic deformation of the metals is responsible for this. At the actual region of contact where the local pressures are very high, the deformation of the metals will be plastic. Near this region, however, where the pressures are smaller the metals will be elastically deformed. When the load is decreased, these stresses will be released and the small movement that results will serve to break the metallic junctions. The area of contact at any given time will, therefore, be determined by the actual load between the surfaces. In the case of a soft plastic metal like indium, however, which shows little elastic recovery, this will not occur, and once the clean surfaces are pressed together they will continue to adhere even when the load is reduced or removed. Similar effects have been observed with gold when its temperature was raised to its softening point.[17] For this reason, measurements of the "coefficient of friction" of an indium slider on a flat steel plate may have little meaning. If, however, the friction is measured as a function of the real area of contact, this difficulty does not arise and consistent results are obtained.

In the experiments described in this paper, the speed of sliding was very low, so that the rise in the surface temperature due to frictional heating

was small. If higher speeds are used, the rise in temperature may be considerable, and a surface softening or local melting may occur. Under these conditions, it is clear that the controlling factor in the frictional behavior of the metals is not their mechanical properties at room temperature, but their properties at the high temperature of sliding.

The analysis outlined has been applied to metals which differ in hardness. It is clear, however, that the same general considerations apply if the surfaces both consist of the same metal, but since both surfaces are torn, it is not easy to evaluate the ploughing and shearing terms separately. The discussion and experiments have been confined to metals, but we may expect similar conclusions to hold for many types of non-metallic solids.

Two-Dimensional Boundary Value Problems in Potential Theory

I. S. Sokolnikoff, *University of Wisconsin, Madison, Wisconsin*

AND

R. D. Specht, *University of Florida, Gainesville, Florida*

(Received November 11, 1942)

A solution of the problem of Dirichlet for a two-dimensional region that can be mapped conformally on a circle is given by the formula of Schwarz. This formula is specialized to yield a complete solution of the torsion problem of St. Venant, and it is demonstrated that the results obtained formally by R. M. Morris are deducible rigorously from the general results of N. Muschelisvili. It is shown that the solution of the torsion problem for a prism whose cross section is the inverse of an ellipse, offered by T. J. Higgins, can be obtained more easily by utilizing the method outlined in this paper rather than by following the procedure of R. M. Morris.

INTRODUCTION

In a recent paper in this journal T. J. Higgins[1] considered the problem of torsion of a cylinder whose cross section is the inverse of an ellipse with respect to its center. Higgins applied a method of solution developed by R. M. Morris,[2] in the process of which he obtained expressions for the complex torsion function and for the twisting moment in the form of infinite series of exponential functions. These series Higgins succeeded in summing. The fact that the final results appear in closed form indicates that the problem under consideration should be capable of solution without intervention of infinite series, and hence with less calculational effort.

In 1938 one of the present authors[3] called attention to a simple general method of solution of problems in potential theory which is overlooked by many investigators dealing with such technically important problems as those on the flow of fluids past obstacles (airfoil problems), flexure and torsion problems of St. Venant, and a variety of problems in harmonic analysis.

It will be shown in this paper that the method of solution proposed by Morris, and utilized by Higgins, is inherently unwieldy since it depends on a representation of a certain mapping function in an infinite series of exponential functions. The connection of the formal procedure developed by Morris with the rigorous and simple method employed by N. Muschelisvili and others[4] will be dealt with completely elsewhere, and it will be merely demonstrated here how results obtained by Higgins follow immediately, in closed form,

[1] T. J. Higgins, J. App. Phys. **13**, 457 (1942).

[2] R. M. Morris, Math. Ann. **116**, 374 (1939); Math. Ann. **117**, 31 (1940–41); Proc. Math. Soc. London [2] **46**, 81 (1940).

[3] I. S. Sokolnikoff and E. S. Sokolnikoff, Bull. Am. Math. Soc. **44**, 384 (1938).

[4] N. Muschelisvili, Rendiconti, Acc. dei Lincei [6] **9**, 295 (1929). For an extensive list of references to recent work utilizing this method in harmonic and biharmonic analysis see I. S. Sokolnikoff, Bull. Am. Math. Soc. **48**, 539 (1942).

upon application of the rudiments of the theory of residues.

Because of the great usefulness of the function-theoretic methods of approach to technical problems, and because of the lack of familiarity on the part of engineers and physicists with such methods, we give in the next section a brief outline of the basic ideas underlying one such method, and apply it to obtain the general solution of the torsion problem of St. Venant. The concluding section of this paper consists of the application of these general considerations to the particular problem treated by Higgins and verifies the correctness of his results.

SECTION 2. GENERAL SOLUTION OF THE PROBLEM OF DIRICHLET

Let it be required to determine a function $u(\xi, \eta)$ harmonic in the interior of the unit circle $|\zeta|=1$ ($\zeta=\xi+i\eta$), which on the boundary γ of the circle assumes prescribed values

$$u=f(\theta), \quad 0\leq\theta\leq 2\pi, \tag{1}$$

where $f(\theta)$ is a continuous real function of the angular variable θ and has period 2π. We shall find it convenient to denote the points on the boundary of the unit circle by $\sigma=e^{i\theta}$. Let the complex conjugate of the function $u(\xi, \eta)$ be denoted by $v(\xi, \eta)$; then the function

$$\Phi(\zeta)=u(\xi, \eta)+iv(\xi, \eta)$$

is an analytic function of the complex variable ζ for $|\zeta|<1$. Furthermore, if $\Phi(\zeta)$ is continuous up to and on the contour γ, the boundary condition (1) can be written in the form

$$\Phi(\sigma)+\bar{\Phi}(\bar{\sigma})=2f(\theta) \text{ on } \gamma, \tag{2}$$

where bars over letters denote, as usual, the conjugate complex values. If we multiply both members of (2) by $(1/2\pi i)(d\sigma/\sigma-\zeta)$, where ζ is any point interior to the unit circle, and integrate over γ, we obtain

$$\frac{1}{2\pi i}\int_\gamma \frac{\Phi(\sigma)}{\sigma-\zeta}d\sigma+\frac{1}{2\pi i}\int_\gamma \frac{\bar{\Phi}(\bar{\sigma})}{\sigma-\zeta}d\sigma=\frac{1}{\pi i}\int_\gamma \frac{f(\theta)}{\sigma-\zeta}d\sigma. \tag{3}$$

The first of the integrals in the left-hand member of (3), by Cauchy's integral formula, equals $\Phi(\zeta)$ while the second* is equal to $\bar{\Phi}(0)$. Thus (3) yields the formula

$$\Phi(\zeta)=\frac{1}{\pi i}\int_\gamma \frac{f(\theta)}{\sigma-\zeta}d\sigma+\text{const.} \tag{4}$$

The formula (4) reduces the solution of the problem of Dirichlet for a circle to a quadrature.

Consider now a region R bounded by a simple closed curve C drawn in the complex z plane ($z=x+iy$), and let it be required to determine a function $\varphi(x, y)$ which is harmonic in R and which assumes on the boundary C continuous real values $g(x, y)$. Then

$$\varphi=g(x, y) \text{ on } C, \tag{5}$$

and if $\psi(x, y)$ is the complex conjugate of $\varphi(x, y)$, the function

$$F(z)=\varphi(x, y)+i\psi(x, y)$$

is analytic in the region R. If $F(z)$ is continuous in the closed region $R+C$, then the boundary condition (5) can be written as

$$F(z)+\bar{F}(\bar{z})=2g(x, y) \text{ on } C. \tag{6}$$

We introduce next a function $z=\omega(\zeta)$ mapping the region R conformally on the region bounded by the unit circle γ in the ζ plane; then the function

$$F[\omega(\zeta)]\equiv\Phi(\zeta)$$

surely is an analytic function of ζ for $|\zeta|<1$. It follows from (6) that the real part of $\Phi(\zeta)$ assumes on $|\zeta|=1$ the values

$$g\left(\frac{\omega(\sigma)+\bar{\omega}(\bar{\sigma})}{2}, \frac{\omega(\sigma)-\bar{\omega}(\bar{\sigma})}{2i}\right)\equiv f(\theta) \text{ on } \gamma, \tag{7}$$

since

$$\sigma=e^{i\theta} \quad \text{and} \quad \bar{\sigma}=e^{-i\theta}.$$

Thus, the problem of determining the function $F(z)$ is reduced to the calculation of the function $\Phi(\zeta)$ from formula (4) in which the function $f(\theta)$ is given by (7).

---

* Note that since $\Phi(\zeta)$ is analytic in $|\zeta|<1$ and continuous in $|\zeta|\leq 1$,

$$\bar{\Phi}(\bar{\sigma})=\bar{\Phi}(1/\sigma)=\sum_{n=0}^{\infty} a_n\sigma^{-n}.$$

Consequently

$$\int_\gamma \sum_{n=0}^{\infty}\frac{a_n}{\sigma^n(\sigma-\zeta)}d\sigma=\sum_{n=0}^{\infty}\int_\gamma \frac{a_n}{\sigma^n(\sigma-\zeta)}d\sigma=a_0=\bar{\Phi}(0).$$

The advantage of the method of solution just outlined, aside from its remarkable simplicity, is that it makes available the theory of residues, which in many instances enables one to obtain solutions in closed form and with a minimum of calculational effort.

We proceed to specialize the foregoing considerations in order to obtain the general solution of the torsion problem of St. Venant. The torsion problem of St. Venant for a right cylinder whose normal section is a simple closed curve C is solved whenever one determines the function $\psi(x, y)$ which is harmonic in the region R bounded by C, and which satisfies the boundary condition

$$\psi=\tfrac{1}{2}(x^2+y^2)=\tfrac{1}{2}z\bar{z} \text{ on } C. \tag{8}$$

It is customary to define the complex torsion function $G(z)$ by the expression

$$G(z)=\varphi+i\psi,$$

where φ is the complex conjugate of ψ, and represents the distortion of the cross sections of the cylinder. If the region R is mapped conformally on the unit circle γ in the ζ plane, with the aid of the mapping function $z=\omega(\zeta)$, then

$$\varphi+i\psi=G[\omega(\zeta)]\equiv\Omega(\zeta),$$

and it is clear from (8) that the imaginary part of the analytic function $\Omega(\zeta)$ satisfies the condition

$$\psi=\tfrac{1}{2}\omega(\sigma)\bar{\omega}(\bar{\sigma})\equiv f(\theta) \text{ on } |\zeta|=1. \tag{9}$$

Accordingly, formula (4) becomes available for the determination of the complex torsion function provided that we replace** in (4) $\Phi(\zeta)$ by

$$(1/i)\Omega(\zeta)=\psi-i\varphi,$$

and $f(\theta)$ by the function defined in (9). Thus

$$\frac{1}{i}\Omega(\zeta)=\frac{1}{\pi i}\int_\gamma \frac{1}{2}\frac{\omega(\sigma)\bar{\omega}(\bar{\sigma})}{\sigma-\zeta}d\sigma+\text{const.},$$

or

$$\Omega(\zeta)=\frac{1}{2\pi}\int_\gamma \frac{\omega(\sigma)\bar{\omega}(1/\sigma)}{\sigma-\zeta}d\sigma+\text{const.}, \tag{10}$$

since $\bar{\sigma}=1/\sigma$ on γ.

It is a simple matter to calculate the torsional rigidity of the cylinder in terms of the variables of the ζ plane. Indeed, the torsional rigidity D is given by the formula

$$\begin{aligned} D&=\mu\int\int_R (x^2+y^2)dxdy \\ &\quad+\mu\int\int_R\left(x\frac{\partial\varphi}{\partial y}-y\frac{\partial\varphi}{\partial x}\right)dxdy \qquad (11)\\ &=\mu I_0+\mu D_0, \end{aligned}$$

where I_0 is the polar moment of inertia of the normal cross section of the prism, D_0 stands for the second integral in the right-hand member of (11), and μ is the shearing modulus.

An elementary calculation, making use of Green's theorem, yields[5]

$$I_0=\frac{1}{4i}\int_\gamma[\bar{\omega}(1/\sigma)]^2\omega(\sigma)d\omega(\sigma), \tag{12}$$

$$D_0=-\frac{1}{4}\int_\gamma[\Omega(\sigma)+\bar{\Omega}(1/\sigma)]d[\omega(\sigma)\bar{\omega}(1/\sigma)]. \tag{13}$$

Since the shearing stresses X_z and Y_z are given by the expressions

$$X_z=\mu\tau[(\partial\varphi/\partial x)-y], \quad Y_z=\mu\tau[(\partial\varphi/\partial y)+x],$$

where τ is the angle of twist per unit length of the cylinder, we can write

$$\begin{aligned} X_z-iY_z&=\mu\tau\left(\frac{\partial\varphi}{\partial x}-i\frac{\partial\varphi}{\partial y}-y-ix\right)\\ &=\mu\tau\left[\left(\frac{\partial\varphi}{\partial x}+i\frac{\partial\psi}{\partial x}\right)-i(x-iy)\right]. \end{aligned}$$

But

$$dG/dz=(\partial\varphi/\partial x)+i(\partial\psi/\partial x),$$

and the foregoing expression assumes the form

$$X_z-iY_z=\mu\tau[G'(z)-i\bar{z}].$$

Setting $z=\omega(\zeta)$ and recalling the definition $\Omega(\zeta)=G[\omega(\zeta)]$, we get a compact formula for the stresses,

$$X_z-iY_z=\mu\tau\left[\frac{\Omega'(\zeta)}{\omega'(\zeta)}-i\bar{\omega}(\bar{\zeta})\right]. \tag{14}$$

** We recall that the boundary condition (7) was imposed on the real part of the function $\Phi(\zeta)$.

[5] These formulas are due to N. Muschelisvili, reference 4; see also, I. S. Sokolnikoff, *Mathematical Theory of Elasticity* (Brown University, 1941), 394 pp., formulas (44–7) and (44–8).

The twisting moment M is given by

$$M=\mu\tau(I_0+D_0). \tag{15}$$

Formulas (10), (14), and (15) furnish all the necessary information pertaining to action of twisted beams.

If the mapping function $\omega(\zeta)$ is expanded in a power series in ζ, and if

$$z=\omega(\zeta)=\sum_{m=0}^{\infty}a_m\zeta^m \tag{16}$$

is inserted in (10), (12), and (13), one obtains at once the expressions given by Morris.[2]

In order to indicate how the formalism of Morris can be rigorously justified, we derive an expression for the complex torsion function used by Higgins.[6]

We observe from (16) that

$$\begin{aligned}\omega(\sigma)\bar{\omega}(1/\sigma)&=\sum_{m=0}^{\infty}a_m\sigma^m\sum_{m=0}^{\infty}\bar{a}_m\sigma^{-m}\\&=\sum_{n=0}^{\infty}b_n\sigma^n+\sum_{n=1}^{\infty}\bar{b}_n\sigma^{-n},\end{aligned} \tag{17}$$

where

$$b_n=\sum_{m=0}^{\infty}a_{n+m}\bar{a}_n.$$

Inserting from (17) in the integrand of (10) we obtain (without calculations)

$$\Omega(\zeta)=i\sum_{n=0}^{\infty}b_n\zeta^n,$$

since $\sum_{n=0}^{\infty}b_n\sigma^n$ is analytic in the unit circle and

$$\int_\gamma\frac{d\sigma}{\sigma^n(\sigma-\zeta)}=0 \text{ for } n=1, 2, \cdots.$$

The derivation of the expression for the moment M is equally simple.

R. M. Morris gives a formal solution of the torsion problem for those cases in which the coefficients a_m in (16) are known. However, if the mapping function $\omega(\zeta)$ is originally given in closed form, it may be easier to proceed directly from formulas (10), (12), and (13) rather than expand $\omega(\zeta)$ in a power series and then deal with the resulting infinite series. We illustrate this by giving an elegant solution of the problem considered by Higgins.

SECTION 3. TORSION OF A PRISM WHOSE CROSS SECTION IS THE INVERSE OF AN ELLIPSE

The mapping function for the inverse of an ellipse with respect to its center is[7]

$$z=c\sec(w+ik),\quad \zeta=e^{iw}$$

or

$$z=\omega(\zeta)=\frac{2c\zeta e^k}{\zeta^2+e^{2k}}.$$

In this case Eq. (10) becomes

$$\begin{aligned}\Omega(\zeta)&=\frac{2c^2}{\pi}\int_\gamma\frac{\sigma^2d\sigma}{(\sigma^2+e^{2k})(\sigma^2+e^{-2k})(\sigma-\zeta)}+\text{const.}\\&=-4c^2i(R_1+R_2)+\text{const.},\end{aligned}$$

where R_1 and R_2 are the residues of the integrand at $\sigma=ie^k$ and $\sigma=-ie^k$, respectively. We have

$$\begin{aligned}R_1&=[\sigma^2(\sigma+ie^k)^{-1}(\sigma^2+e^{-2k})^{-1}(\sigma-\zeta)^{-1}]_{\sigma=ie^k}\\&=\frac{ie^k}{4(\zeta-ie^k)\sinh(2k)},\end{aligned}$$

$$R_2=\frac{-ie^k}{4(\zeta+ie^k)\sinh(2k)},$$

and hence

$$\Omega=\varphi+i\psi=c^2\operatorname{csch}(2k)\tan(w+ik),$$

which is Eq. (16) of T. J. Higgins' paper. (The constant in (10) has been taken equal to $-ic^2\operatorname{csch}(2k)$.) Equation (12) for the moment of inertia I_0 takes the form

$$\begin{aligned}I_0&=4c^2i\int_\gamma\sigma^3(\sigma^2-e^{2k})(\sigma^2+e^{2k})^{-3}(\sigma^2+e^{-2k})^{-2}d\sigma\\&=-8\pi c^4(R_3+R_4),\end{aligned}$$

where R_3 and R_4 are the residues of the integrand at $\sigma=ie^{-k}$ and $\sigma=-ie^{-k}$, respectively. The residues are:

$$\begin{aligned}R_3&=(d/d\sigma)[\sigma^3(\sigma^2-e^{2k})(\sigma^2+e^{2k})^{-3}(\sigma+ie^{-k})^{-2}]_{\sigma=ie^k}\\&=-\operatorname{csch}^4(2k)(2+\cosh 4k)/16=R_4,\end{aligned}$$

[6] T. J. Higgins, reference 1, formula (3) on p. 457. This formula appears on p. 387 of Morris' paper in Math. Ann. **116** (1939).

[7] Cf. T. J. Higgins, reference 1, formula (1).

and therefore

$$I_0=\pi c^4(2+\cosh 4k)\ \mathrm{csch}^4\ 2k.$$

Similarly from (13) we get

$$D_0=-i4c^4\ \mathrm{csch}\ (2k)\int_\gamma \sigma(1-\sigma^4)^2 \times(\sigma^2+e^{2k})^{-3}(\sigma^2+e^{-2k})^{-3}d\sigma$$

$$=8\pi c^4\ \mathrm{csch}\ (2k)(R_5+R_6),$$

in which R_5 and R_6 are the residues at $\sigma=ie^{-k}$ and $\sigma=-ie^{-k}$. We find that

$$R_5=\tfrac{1}{2}(d^2/d\sigma^2)[\sigma(1-\sigma^4)^2(\sigma^2+e^{2k})^{-3} \times(\sigma+ie^{-k})^{-3}]_{\sigma=ie^{-k}}$$

$$=-(\mathrm{csch}^3\ 2k)/8=R_6,$$

and hence

$$D_0=-2\pi c^4\ \mathrm{csch}^4\ 2k.$$

The twisting moment, as given by (15), is

$$M=\mu\tau(I_0+D_0)=\mu\tau\pi c^4(2\ \mathrm{csch}^2\ 2k+\mathrm{csch}^4\ 2k),$$

which is formula (31) of T. J. Higgins' paper.

The shearing stresses may be found either from the relations

$$X_z=\mu\tau\partial\Psi/\partial y,\quad Y_z=-\mu\tau\partial\Psi/\partial x,$$

$$\Psi=\psi-\tfrac{1}{2}(x^2+y^2),$$

or from Eq. (14).

Probable X-Ray Mass Absorption Coefficients for Wave-Lengths Shorter Than the *K* Critical Absorption Wave-Length

JOHN A. VICTOREEN
The Victoreen Instrument Company, Cleveland, Ohio

(Received December 11, 1942)

Absorption coefficients of all elements may be calculated, from short wave-lengths up to the K critical absorption wave-length by the expression:

$$\mu/\rho=\alpha\lambda^3Z^2(2Z/A)-\beta\lambda^4Z^5(2Z/A)+\sigma_eN_0(Z/A).$$

This formula holds for all elements when suitable values for α and β are chosen. Factors α and β are related to the atomic number, Z, by the expressions $\alpha=(aZ^2+bZ-c)$, and $\beta=(dZ^2-eZ+f)$. Different values of the constants a, b, c, d, e, and f are required for each side of the critical absorption wave-lengths and for either side of $Z=5$, and are given for the short wave-length side of the K critical absorption wave-lengths. The values of $\alpha Z^2(2Z/A)$ and $\beta Z^5(2Z/A)$ computed for all elements, are shown in the tables. The calculated mass absorption coefficients of a few elements are also furnished together with comparison of calculated mass absorption coefficients with published experimental data. No anomalies were found and the average agreement is of the order of 1 to 2 percent for all elements and all wave-lengths on the short wave-length side of the K critical absorption wave-length. Values for the region between the K and L_1 critical absorption wave-lengths will be published later.

INTRODUCTION

NUMEROUS empirical expressions have been suggested for calculation of mass and atomic absorption coefficients. None, however, has represented all elements nor covered wide ranges of wave-lengths.

The prevailing belief has been that the rate of change of the absorption coefficient increases up to the critical absorption wave-length, and hence most empirical expressions have been of the following type:

$$\mu=C\lambda^mZ^n+b. \qquad (1)$$

A few examples, each intended to cover only a limited range of atomic numbers or wave-lengths are:

Siegbahn,[1] $\mu_m=C'\lambda^n$ for a given Z,
Bragg and Pierce,[2] $\mu_a=CZ^4\lambda^{5/2}$,

[1] M. Siegbahn, Physik. Zeits. **15**, 753 (1914).
[2] W. H. Bragg, Phil. Mag. **29**, 407 (1915).

Hull and Rice,[3] $\mu/\rho_{al}=14.9\lambda^3$
$+0.12$ for aluminum,
Walter,[4] $\tau_a=2.64\times10^{-26}Z^{3.94}$,
Richtmyer,[5] $\mu_a=2.29\times10^{-27}Z^4$,
Dershem and Schein,[6] $\mu_a=1.65\times10^{-23}Z^{4.4}$.

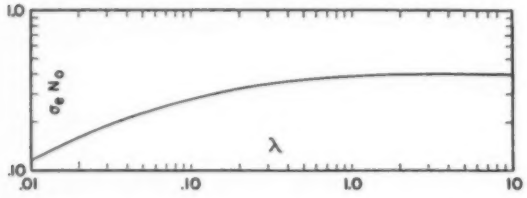

FIG. 1. Values of $\sigma_e N_0$ calculated from the Klein-Nishina formula.

Earlier expressions assumed the scattering coefficient [b in (1)] to be about 0.15 and independent of wave-length. Classical theory, however, led to the following expression for scattering per electron:

$$\sigma=\frac{8}{3}\cdot\frac{\pi e^4}{m^2c^4}. \tag{2}$$

But this does not agree with experimental data; these indicate a scattering coefficient which varies with wave-length.

Compton,[7] Dirac,[8] and Klein and Nishina[9] modified the classical expression by taking into account the relativistic mass of the electron. Their expressions led to the classical value at the longer wave-lengths, but differ considerably at short wave-lengths. Only the Klein and Nishina formula has given good agreement with experiment. However, satisfactory agreement has been obtained only on elements of low atomic number and at short wave-lengths, for only under these conditions is the contribution of photoelectric absorption sufficiently small to make any error in its estimation of negligible importance.

The expression suggested by Klein and Nishina is:

$$\sigma_e=\frac{\pi e^4}{m^2c^4}\cdot 2\left\{\frac{1+\alpha}{\alpha^2}\left[\frac{2(1+\alpha)}{1+2\alpha}-\frac{1}{\alpha}\log_e(1+2\alpha)\right]+\frac{1}{2\alpha}\log_e(1+2\alpha)-\frac{1+3\alpha}{(1+2\alpha)^2}\right\}. \tag{3}$$

Here $\alpha=h\nu/mc^2$ and $\sigma/\rho=\sigma_e N_0(Z/A)$ with:

σ_e—the scattering per electron,
N_0—Avogadro number,
Z—atomic number,
A—atomic weight,
σ/ρ—the mass scattering coefficient,
e—the electronic charge,
m—the electronic mass,
c—the velocity of light,
h—Planck's constant.

A graph of values of $\sigma_e N_0$ obtained from the Klein-Nishina formula for various wave-lengths is shown in Fig. 1.

Assuming that the scattering coefficients predicted by the Klein and Nishina formula will hold also for higher atomic numbers, an empirical expression has been derived, by means of which the mass photoelectric absorption coefficient may be calculated for any element. Empirical

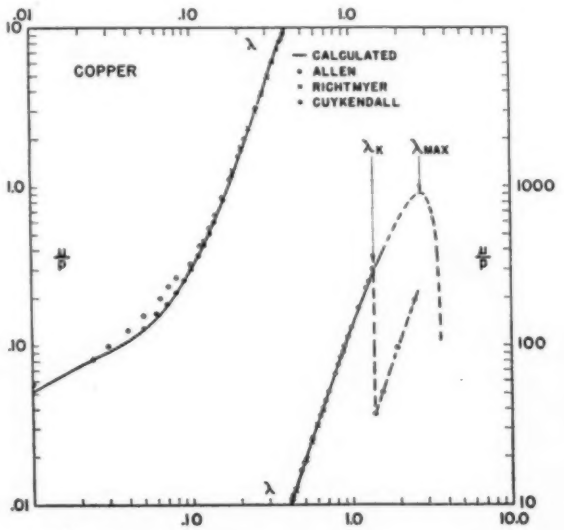

FIG. 2. Mass absorption coefficients of copper. Scale for μ/ρ on left for first part of curve and on right for second part of curve.

[3] A. W. Hull and M. Rice, Phys. Rev. **8**, 326 (1916).
[4] B. Walter, Forts. a.d. Geb. d. Roentgen **35**, 929, 1308 (1927).
[5] F. K. Richtmyer, Phys. Rev. **18**, 13 (1921).
[6] E. Dershem and M. Schein, Phys. Rev. **37**, 1238 (1931).
[7] A. H. Compton, Phys. Rev. **21**, 483 (1923).
[8] P. A. M. Dirac, Proc. Roy. Soc. **101**, 405 (1927).
[9] O. Klein and Y. Nishina, Zeits. f. Physik **52**, 853 (1928).

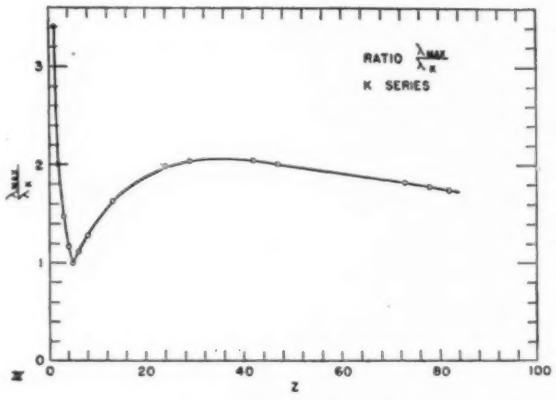

FIG. 3. Ratio of the wave-length of maximum absorption to critical absorption wave-length.

data thus obtained, support the values predicted by the Klein and Nishina formula, for the calculated mass absorption coefficients agree with experimental data within the apparent observational error.

EMPIRICAL EQUATIONS

Previous expressions of the type of Eq. (1) can be used to represent the change of the absorption coefficient over a small range of wave-lengths and atomic numbers. When applied to wide ranges of wave-length they lead to values of μ/ρ which are increasingly higher than experimentally determined values, particularly in the region approaching the critical absorption wave-length.

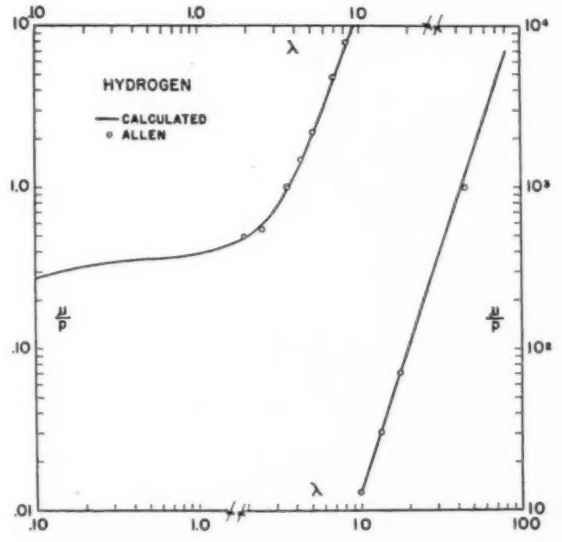

FIG. 4. Mass absorption coefficients of hydrogen.

Richtmyer[5] investigated a number of elements in an attempt to determine the variation of μ/ρ with λ. He concluded: "The linear relation established by Hull and Rice between the mass absorption coefficient and λ^3, $\mu/\rho = F\lambda^3 + \sigma/\rho$, holds accurately for these substances until as λ is increased, the characteristic limit is approached, when the values of μ/ρ are increasingly too small" (referring to his measured values). Other published data show this effect but it appears to have been discounted by many observers. The decrease in the rate of change of μ/ρ, at values of λ approaching the critical absorption wave-length, is particularly evident in the experimentally determined values given in Allen's tables.

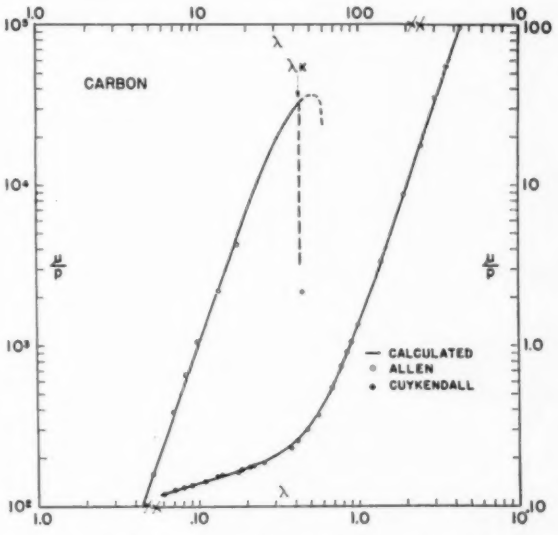

FIG. 5. Mass absorption coefficients of carbon.

All available experimental data by different observers have been investigated by methods of graphic analysis in an effort to obtain an empirical expression which will represent more accurately, the value of μ/ρ for any wave-length up to or near the critical absorption wave-length, and the relation of μ/ρ to atomic number. Equations (4) and (5) are the result of this investigation.

$$\tau/\rho = \alpha Z^2\lambda^3(2Z/A) - \beta Z^5\lambda^4(2Z/A), \qquad (4)$$

the values of α and β changing at each critical wave-length. Z is the atomic number; A, atomic weight; and λ, wave-length in angstroms. The

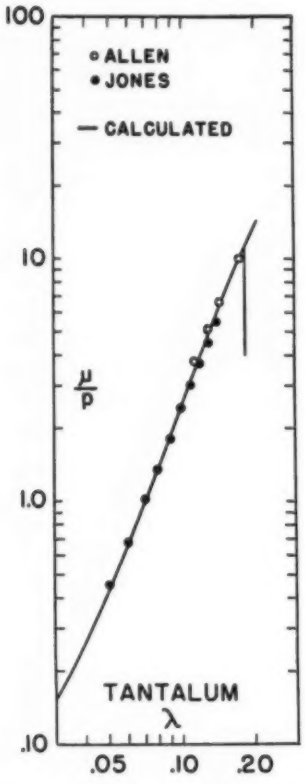

FIG. 6. Mass absorption coefficients of tantalum.

quantity $2Z/A$ corrects for the variation in the number of atoms per gram due to the presence of isotopes.

The mass absorption coefficient is the sum of the mass photoelectric absorption coefficient from Eq. (4) and the mass scattering coefficient from Eq. (3). Therefore:

$$\frac{\mu}{\rho}=\frac{\tau}{\rho}+\frac{\sigma}{\rho}=\alpha Z^2\lambda^3\frac{2Z}{A}-\beta Z^5\lambda^4\frac{2Z}{A}+\sigma_e N_0\frac{Z}{A}. \quad (5)$$

For elements 1, 2, 3, 4, and 5, empirically suggested values of α and β on the short wave-length side of the K critical absorption wave-length are:

$$\alpha_K=0.00650Z,$$
$$\beta_K=2.35\times10^{-6}.$$

For elements 5 and higher:

$$\alpha_K=(aZ^2+bZ-C)$$
$$=(0.0000400Z^2+0.00728Z-0.0114), \quad (6)$$

$$\beta_K=(dZ^2-eZ+f)$$
$$=(0.000380Z^2-0.00152Z+2.35)\times10^{-6}. \quad (7)$$

The values of α_K and β_K and a, b, c, d, e, and f were selected, after careful consideration, as best representing all available experimental data.

Equation (5) indicates that as the wave-length is increased, a point will be reached, at which rate of change of absorption coefficient with wave-length will decrease as the critical absorption wave-length is approached. The effect is shown in Fig. 2. It is found that if the values are projected beyond the critical absorption wave-length, the rate of change finally becomes zero, and the absorption coefficient is maximum at a wave-length which is 1.0 to 2.0 times the critical absorption wave-length, depending on atomic number.

Figure 3 shows the ratio $\lambda\,\max/\lambda_K$ plotted against atomic number.

Coefficients of hydrogen, carbon, lead, and tantalum (Figs. 4, 5, 6, and 7), as well as coefficients of copper (Fig. 2), are representative of the entire range of atomic numbers. The calculated values are consistent with experiment at all values of atomic number and at all wave-lengths.

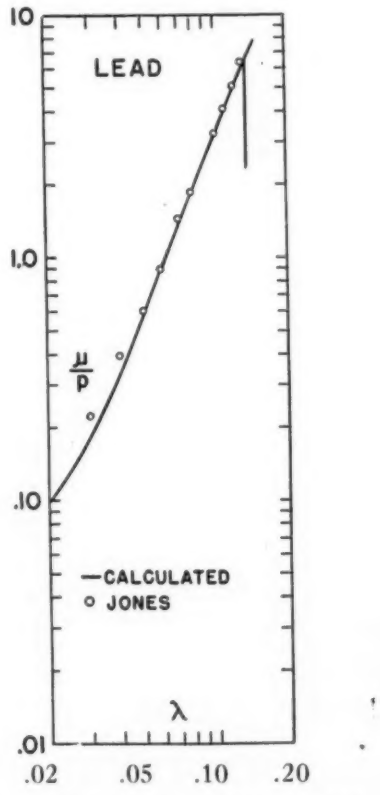

FIG. 7. Mass absorption coefficients of lead.

TABLE I. Values of C, D, Z/A, and λ for the elements. Wave-length in angstroms. [For Eq. (8).]

Z	C	D	Z/A	Limit λ_K	Z	C	D	Z/A	Limit λ_K
1	01289	4.662×10^{-6}	0.9922		47	808.8	624.8	0.4356	0.4844
2	05197	75.16×10^{-6}	0.4997	504.2	48	854.1	692.2	0.4270	0.4631
3	0.1517	493.6×10^{-6}	0.4322		49	904.3	768.6	0.4269	0.4429
4	0.3689	2133×10^{-6}	0.4434		50	952.3	842.0	0.4212	0.4239
5	0.6006	006791	0.4621	64.3	51	1010	941.9	0.4188	0.4060
6	1.211	01830	0.5000	43.5	52	1042	1017	0.4074	0.3892
7	2.034	03963	0.4997	31.1	53	1140	1163	0.4175	0.3734
8	3.161	0.07739	0.5000	23.5	54	1194	1273	0.4112	0.3577
9	4.404	0.1324	0.4736		55	1258	1401	0.4140	0.3440
10	6.487	0.2353	0.4954		56	1330	1548	0.4076	0.3307
11	8.503	0.3661	0.4783		57	1421	1725	0.4103	0.3181
12	11.65	0.5876	0.4934	9.496	58	1524	1928	0.4139	0.3062
13	14.69	0.8583	0.4820	7.935	59	1621	2140	0.4186	0.2951
14	19.19	1.286	0.4989	6.731	60	1700	2339	0.4158	0.2845
15	23.93	1.768	0.4835	5.774	61	1808	2590	0.4178	
16	29.49	2.538	0.4990	5.008	62	1879	2804	0.4121	0.2644
17	34.34	3.314	0.4794	4.383	63	1990	3090	0.4144	0.2548
18	38.80	4.174	0.4506	3.865	64	2061	3325	0.4068	0.2462
19	49.47	5.903	0.4859	3.431	65	2174	3649	0.4082	0.2376
20	60.08	7.907	0.4990	3.064	66	2274	3968	0.4062	0.2301
21	65.21	9.430	0.4656	2.751	67	2407	4364	0.4097	0.2226
22	78.06	12.36	0.4592	2.491	68	2540	4784	0.4116	
23	84.49	14.60	0.4514	2.263	69	2639	5160	0.4073	0.2085
24	98.72	18.54	0.4614	2.065	70	2748	5571	0.4045	0.2016
25	111.2	22.65	0.4551	1.891	71	2886	6074	0.4057	0.1951
26	129.0	28.41	0.4656	1.739	72	3007	6564	0.4031	0.1901
27	143.0	33.96	0.4580	1.604	73	3144	7115	0.4024	0.1836
28	167.6	42.85	0.4770	1.483	74	3285	7701	0.4021	0.1782
29	178.9	49.09	0.4561	1.377	75	3434	8343	0.4025	0.1735
30	200.7	59.01	0.4588	1.280	76	3543	8911	0.3968	0.1675
31	215.5	67.79	0.4446	1.190	77	3719	9687	0.3987	0.1620
32	236.9	79.60	0.4407	1.116	78	3882	10460	0.3995	0.1577
33	262.2	93.36	0.4405	1.042	79	4070	11354	0.4006	0.1532
34	280.6	106.8	0.4305	0.9777	80	4233	12212	0.3987	0.1489
35	313.7	127.0	0.4379	0.9180	81	4367	13028	0.3963	0.1444
36	337.0	144.9	0.4301	0.8637	82	4537	13998	0.3957	0.1404
37	370.5	168.8	0.4330	0.8141	83	4737	15098	0.3971	0.1367
38	404.7	195.3	0.4336	0.7683	84	4980	16403	0.4565	
39	444.0	226.6	0.4385	0.7255	85	5180	17623	0.4009	
40	481.8	259.8	0.4385	0.6873	86	5117	17978	0.3873	
41	522.7	297.4	0.4394	0.6515	87	5458	19798	0.3901	
42	562.4	337.3	0.4375	0.6184	88	5685	21284	0.3911	
43	609.6	385.4	0.4396		89	5889	22748	0.3886	
44	646.1	429.9	0.4326	0.5584	90	6083	24240	0.3877	0.1127
45	702.9	491.9	0.4372	0.5330	91	6181	25404	0.3888	
46	745.9	548.5	0.4311	0.5079	92	6512	27240	0.3863	0.1065
					H_2O	2.808	0.06873	0.5549	23.5
					Air	2.768	0.1017	0.4993	3.86

The values of λ_K were taken from Compton and Allison (reference 12).

TABLE II. Values of $\sigma_e N_0$. Wave-length in angstroms. Calculated from Klein-Nishina formula.

λ	$\sigma_e N_0$	λ	$\sigma_e N_0$	λ^3	λ^4	λ	$\sigma_e N_0$
0.01	0.113	0.10	0.279	0.001000	0.0001000	1.0	0.387
.012	.125	.12	.293	.001728	.0002073	1.2	.390
.015	.140	.15	.309	.003375	.0005062	1.5	.394
.02	.160	.20	.325	.008000	.001600	2.0	.395
.025	.175	.25	.337	.01562	.003906	2.5	.396
.03	.188	.30	.346	.02700	.008100	3.0	.397
.04	.210	.40	.357	.06400	.02560	4.0	.397
.05	.226	.50	.365	.1250	.06250	5.0	.398
.06	.240	.60	.371	.2160	.1296	6.0	.399
.08	.262	.80	.380	.5120	.4096	8.0	.400

The values of λ^3 and λ^4 are included for convenience and may be used in the other ranges of wave-length by suitably moving the decimal point. The values of the physical constants used in computing $\sigma_e N_0$ were the same as used by Cuykendall (reference 11) and Jones (reference 10):

$N_0 = 6.06\times10^{23}$
$e = 4.767\times10^{-10}$ e.s.u.
$m = 0.9038\times10^{-27}$ g
$c = 2.998\times10^{10}$ cm/sec.
$h = 6.542\times10^{-27}$ erg/sec.

Some of the values of $\sigma_e N_0$ have been interpolated with an accuracy of better than 1 percent.

From Eq. (5):

$$\mu/\rho = C\lambda^3 - D\lambda^4 + \sigma_e N_0 (Z/A), \qquad (8)$$

where

$$C = \alpha Z^2 (2Z/A),$$
$$D = \beta Z^5 (2Z/A).$$

Table I shows values of C, D, Z/A, and λ for each element.

Table II gives values of $\sigma_e N_0$ at various wave-lengths.

Table III presents calculated values of mass absorption coefficients of some common elements.

COMPARISON OF CALCULATED VALUES WITH PUBLISHED EXPERIMENTAL DATA

Observers disagree as to the correct values for certain elements and at certain wave-lengths. Since these data are widely distributed in the literature, the commonly used data should be considered separately.

The ratio of μ/ρ observed, to μ/ρ calculated, has therefore been computed for each of the points given by the various observers whose data are most widely used. These values comprise Tables IV, V, VI, and VII.

The data in Table IV represent the latest and probably most reliable values, obtained with a large double crystal spectrometer by Jones[10] and Cuykendall.[11] The values enclosed in parentheses evidently are in error.

The data in Table V were published by Richtmyer.[5]

The data in Table VI on gases and vapors were taken from Compton and Allison[12] and represent the findings of several observers, Allen, Allison and Andrew, Colvert, and Woernle. (The source of each value is represented by the letters in parentheses.) Because of difficulties of measurement, the values on gases and vapors vary considerably. For wave-lengths above 3A the data of Woernle are uniformly about 7 percent higher for all elements. At this point there is an abrupt change, shown in Fig. 8 where

[10] M. T. Jones, Phys. Rev. **50**, 110 (1936).
[11] T. R. Cuykendall, Phys. Rev. **50**, 105 (1936).
[12] A. H. Compton and S. K. Allison, *X-Rays in Theory and Experiment* (D. Van Nostrand Company, New York, 1935).

TABLE III. Calculated mass absorption coefficients. Wave-length in angstroms.

λ	Air	H_2O	H	C	N	O	Al	Cu	Ag	Sn	Ta	Pb
0.010	0564	0627	0.112	0565	0565	0565	0545	0516	0500	0484	0485	0491
0.012	0679	0754	0.135	0680	0680	0680	0657	0623	0605	0589	0600	0613
0.015	0699	0776	0.139	0700	0700	0700	0676	0644	0636	0621	0666	0699
0.020	0798	0887	0.158	0800	0800	0800	0773	0743	0760	0748	0884	0973
0.025	0873	0.0971	0.173	0875	0875	0875	0847	0825	0886	0882	0.1167	0.1346
0.03	0938	0.104	0.186	0940	0940	0940	0911	0905	0.1032	0.1042	0.1547	0.1854
0.04	0.104	0.116	0.208	0.105	0.105	0.105	0.102	0.107	0.1416	0.1472	0.2675	0.3375
0.05	0.112	0.125	0.224	0.113	0.113	0.113	0.110	0.125	0.1956	0.2089	0.4395	0.5690
0.06	0.120	0.133	0.238	0.120	0.120	0.120	0.119	0.1474	0.2711	0.2956	0.6834	0.8934
0.08	0.132	0.1467	0.259	0.131	0.131	0.131	0.134	0.2089	0.5026	0.5633	1.423	1.852
0.10	0.1420	0.1576	0.276	0.1402	0.1410	0.1421	0.1493	0.3012	0.8678	0.9856	2.544	3.247
0.12	0.1510	0.1673	0.290	0.1480	0.1495	0.1514	0.1667	0.4325	1.395	1.593	4.074	5.054
0.15	0.1635	0.1808	0.306	0.1590	0.1618	0.1656	0.1983	0.7197	2.547	2.918	7.133	
0.20	0.1843	0.2026	0.3225	0.1716	0.1782	0.1871	0.2730	1.500	5.611	6.407		
0.25	0.2110	0.2305	0.3345	0.1879	0.2006	0.2180	0.3887	2.756	10.33	11.72		
0.30	0.2466	0.2671	0.3436	0.2057	0.2275	0.2577	0.5567	4.590	16.92	19.03		
0.40	0.3527	0.3759	0.3550	0.2560	0.3080	0.3793	1.090	10.35	35.92	39.54		
0.50	0.5218	0.5492	0.3637	0.3331	0.4347	0.5732	1.958	19.45				
0.60	0.7698	0.8034	0.3708	0.4441	0.6191	0.8576	3.241	32.44				
0.80	1.565	1.619	0.3836	0.8025	1.214	1.776	7.353	71.66				
1.00	2.859	2.954	0.3968	1.385	2.187	3.276	14.01	129.9				
1.2	4.766	4.926	0.4091	2.249	3.626	5.496	23.78	207.5				
1.5	9.024	9.347	0.4344	4.191	6.860	10.46	45.41					
2.0	20.71	21.58	0.4950	9.587	15.83	24.24	103.9					
2.5	39.45	41.39	0.5935	18.39	30.42	46.54	196.0					
3.0	66.69	70.45	0.7405	31.41	51.90	79.27	327.2					
4	134.8	162.3	1.216	73.01	120.1	182.7	720.4					
5	257.2	308.2	2.002	140.0	229.6	346.9	1299					
6	434.0	517.4	3.173	237.9	388.1	582.5	2061					
8	978.9	1155	6.979	545.2	878.7	1301	4006					
10	1816	2120	13.24	1028	1637	2387	6107					
12	2972	3428	22.57	1712	2692	3858						
15	5318	5998	43.66	3160	4858	6743						
20	10679	11470	102.7	6752	9930	12900						
25		17020	198.8	11763	16300	19150						

TABLE IV. Comparison of calculated mass absorption coefficients with experimental data of Cuykendall (reference 11) and Jones (reference 10) for different elements and wave-lengths.

λ	C	Na	Al	K	Ni	Cu	Mo	Ag	Sn	Ta	Pb
0.05	1.007	——	1.019	0.9913	0.9805	1.031	1.059	(1.17)	(1.177)	1.041	1.054
0.06	0.9966	1.018	1.016	1.067	(1.084)	(1.084)	1.021	1.043	1.060	1.007	1.007
0.07	0.9952	1.019	1.033	1.032	1.057	1.038	1.080	1.074	1.041	1.009	(1.103)
0.08	1.000	1.031	1.029	1.061	1.041	1.027	1.059	1.081	1.077	0.9536	0.9875
0.09	1.005	1.029	1.016	1.074	1.005	1.032	1.056	1.072	1.061	0.940	0.9975
0.10	1.008	1.035	1.005	1.046	1.001	1.015	0.9989	1.036	1.034	0.958	1.000
0.11	1.015	1.039	1.004	0.9906	0.9881	1.028	0.9959	0.9747	0.9667	(1.034)	0.9943
0.12	1.018	1.042	1.012	1.007	0.9997	1.004	1.006	0.9770	0.9962	0.925	1.019
0.13	1.016	1.044	1.002	1.017	0.9841	0.9966	0.9802	0.9580	0.9671	(0.911)	1.053
0.14	1.021	1.036	1.028	1.059	1.010	0.9936	0.9792	0.9658	0.9557	(0.909)	
0.16	1.016	1.015	1.017	1.046	0.9558	0.9855	0.9504				
0.184	1.021	1.012	0.9807	1.005	0.9598	0.9725	0.9806				
0.209	1.015	0.9905	0.9624	1.011	0.9725	0.9656					

the calculated values of the mass absorption coefficient of atmospheric air are compared with his data.

In Table VII only a few elements and representative points are selected from the large number of Allen's values given in Compton and Allison.[12] Calculated values agree more closely with Allen's tables over a wide range of elements and wave-lengths, than with those of any other single observer. Below about 0.20A, Allen's published data generally disagree with those of all other observers for all elements, and hence

these have not been used in this paper. However more recent unpublished data just received from S. J. M. Allen, agree excellently with Eq. (5) on all wave-lengths.

COMMENT

Values of constants in Eqs. (6) and (7) are empirical and may be expressed in several other ways; the present form was used in order to avoid possible false interpretation.

Tables I, II, and III were prepared in terms of mass absorption coefficients rather than atomic absorption coefficients because of the practical value of the former.

Similar data for absorption coefficients between the K–L critical absorption limits will be presented later.

Values of atomic weight used in computing Z/A are those compiled by Hubbard.[13]

[13] Hubbard, *Periodic Chart of the Atoms* (W. M. Welch Manufacturing Company, Chicago, Illinois, 1935).

TABLE V. Comparison of calculated mass absorption coefficients with experimental data of Richtmyer (reference 5).

λ	Al	Cu	Mo	Ag	H_2O
0.098					1.052
0.120					1.049
0.135	1.069	1.052	1.077		1.032
0.184	0.9807	1.039	1.004	0.9551	1.026
0.209	0.9533	1.031	0.9820	(0.9377)	1.003
0.234	0.9479	1.006	0.9703	(1.100)	0.9981
0.258	0.9569	0.9976	0.9748	(1.110)	0.9961
0.283	0.9532	0.9938	1.002	1.078	0.9849
0.308	0.9644	0.9856	0.9977	1.074	0.9732
0.332	0.9637	0.9855	1.004	1.065	0.9614
0.356	0.9708	0.9795	0.9855	1.070	0.9526
0.368	0.9709	0.9908	0.9868	1.068	0.9522
0.381	0.9732	0.9812	0.9813	1.071	0.9538
0.393	0.9750	0.9794	0.9756	1.077	0.9490
0.405	0.9733	0.9514	0.9669	1.057	0.9342
0.417	0.9686	0.9699	0.9599	1.094	0.9383
0.430	0.9801	0.9685	0.9448	1.109	0.9356
0.453	0.9820	0.9103	0.9759	1.138	
0.479	0.9782	0.9628	0.9615		
0.503	0.9798	0.9610	0.9858		
0.551	0.9745	0.9745	1.010		
0.600	0.9811	0.9741	1.036		
0.650	0.9972	0.9745			
0.715	0.9984	(0.8697)			
0.743	0.9804				

TABLE VI. Comparison of calculated mass absorption coefficients of gases and vapors with experimental data of various observers.*

	7 N	8 O	10 Ne	18 A	17 Cl	1 H	CCl_4	Air
0.496	0.9317(A)		0.8755(C)	1.081(C)	0.9880(C)	1.199(A)		
0.560			0.923(C)	1.048(C)	0.9792(C)			
0.631	0.9537(A)		0.9505(C)	1.059(C)	0.9878(C)	1.150(A)		
0.709	0.9583(A)		1.024(C)	1.003(C)	0.9956(C)	1.139(A)		
0.885	0.9646(A)					1.120(A)		
1.081	0.9593(A)					1.123(A)		
1.095								0.9229(W)
1.274	1.015(A)					1.098(A)		
1.279								0.9798(W)
1.389	1.020(A)		0.9580(AA)	0.9679(AA)	0.9636(C)	1.098(A)		
1.473								0.9690(W)
1.537	1.025(A)		1.038(AA)	0.9685(AA)	0.9670(C)	1.088(A)		0.9864(W)
1.935	0.981(A)					1.023(A)		0.9808(W)
2.081				0.9719(AA)				
2.287		1.014(W)	1.047(W)	1.011(W)	0.9837(C)	0.8697(A)		0.9996(W)
3.378	1.087(W)	1.049(W)	1.071(W)	1.077(W)			0.8981(W)	1.089(W)
3.592	1.096(W)	1.052(W)	1.066(W)	1.097(W)			0.9323(W)	1.095(W)
3.927	1.053(W)	1.081(W)	1.043(W)	1.122(W)			0.9312(W)	1.083(W)
4.146	1.081(W)	1.096(W)	1.059(W)	1.094(W)			1.007(W)	1.092(W)
4.359	1.075(W)	1.103(W)	1.057(W)	1.094(W)			1.092(W)	1.109(W)
5.166	1.082(W)	1.085(W)	1.050(W)	1.063(W)			1.080(W)	1.111(W)
5.394	1.092(W)	1.105(W)	1.057(W)	1.040(W)			1.067(W)	1.112(W)
6.973	1.082(W)	1.098(W)	1.051(W)	1.017(W)			0.9887(W)	1.122(W)
8.323	1.129(W)	1.093(W)	1.031(W)	0.9398(W)			0.9316(W)	1.097(W)
9.868	1.138(W)	1.102(W)	1.077(W)	0.9237(W)		1.020(A)	0.9265(W)	1.121(W)
13.37	1.081(A)					1.013(A)		
17.67	0.9578(A)					1.011(A)		
44.5						0.892(W)		

* (A) = Allen; (AA) = Allison and Andrew; (C) = Colvert; and (W) = Woernle. Taken from Compton and Allison (reference 12), 522–525 and 800–806.

TABLE VII. Comparison of calculated mass absorption coefficients with experimental data from Allen (reference 12).

λ	C	Al	Cu	Mo	Ag	Sn	Ta	Pb
0.130						1.072	1.021	1.029
0.142				0.9663	1.053	1.051		1.067
0.146					1.049	0.9826	1.011	
0.158		1.006			1.022	1.011		
0.175		0.9925		1.040	1.019	1.012	0.9765	
0.178		1.001						
0.184		1.005			0.9975		1.021	
0.200	1.016	0.9900	1.033	1.048	0.9766	0.9676		
0.220					0.9668	0.9390		
0.260		0.9573	1.027	0.9653	0.9913	0.9815		
0.331					0.9877	0.9971		
0.380		0.9733	0.9402	(0.9178)	0.9904	0.9756		
0.417	0.9580	0.9653	0.9828	0.9762	1.027	1.028		
0.424		0.9723				1.023		
0.476		1.015	0.9810	0.9661	1.085			
0.485		0.9822						
0.497		0.9859	0.9618	1.032				
0.560		0.9723	0.9532					
0.618				1.052				
0.631		0.9983	0.9699					
0.680		0.9789	0.9864					
0.710		1.000	0.9860					
0.780			1.009					
0.814		1.015	1.007					
0.850		1.010	1.001					
0.880			0.9844					
0.900	0.9868		1.001					
0.949			1.007					
1.00		1.007	1.000					
1.23			1.042					
1.29			1.047					
1.38	1.010							
1.53		1.018						
1.93		0.9502						
2.50	0.9679	0.9846						
3.38	1.006							
4.15		(0.9060)						
5.17	1.032							
6.97	1.062	0.9494						
9.87	1.073							
13.3	(0.9534)							
17.6	(0.8871)							

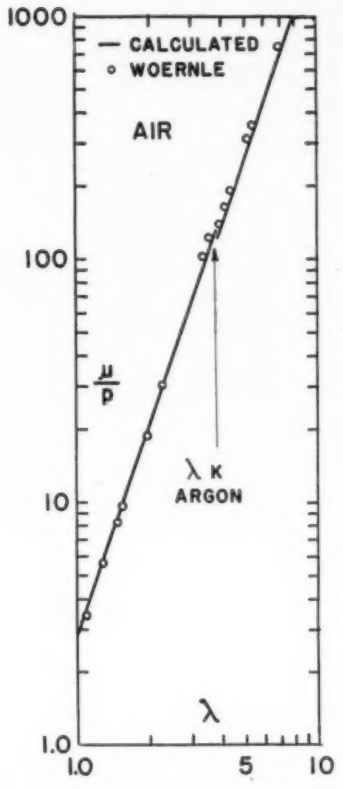

FIG. 8. Mass absorption coefficients of atmospheric air.

CONCLUSIONS

An empirical equation (5) is presented by means of which mass absorption coefficients for all elements may be calculated with an accuracy greater than that obtained experimentally by any single observer over a wide range of elements and wave-lengths.

The calculative method is useful when it is desirable to correlate the absorption for various conditions for which only incomplete data are available, and for elements for which data are not otherwise available.

Evidence exists to support the conclusion that absorption of an element is dependent only on its atomic number Z and is independent of its isotopes except insofar as this affects the number of atoms per gram in the mass absorption coefficient.

Good agreement is obtained with the Klein-Nishina formula for all elements.

The absorption varies continuously from element to element from 1 to 5 and 5 to 92.

The coefficients between the K and L critical absorption wave-lengths follow the same laws as for the region shorter than the K limit with a change in the values of Eqs. (6) and (7), but are not a continuation of the values on the short wave-length side of the K limit multiplied by the ratio λ_{L1}/λ_K, as suggested by Jönsson.[14]

The calculated values may not strictly hold up to the critical absorption wave-length but by graphical evaluation this appears to be true.

[14] E. Jönsson, Thesis, Upsala. See Compton and Allison's, *X-Rays in Theory and Experiment* (D. Van Nostrand Company, New York, 1935).